JVI Journals.ASM.org

Methyltransferase-Defective Avian Metapneumovirus Vaccines Provide Complete Protection against Challenge with the Homologous Colorado Strain and the Heterologous Minnesota Strain

Jing Sun,[a,e] Yongwei Wei,[a] Abdul Rauf,[b] Yu Zhang,[a] Yuanmei Ma,[a] Xiaodong Zhang,[a] Konstantin Shilo,[c] Qingzhong Yu,[d] Y. M. Saif,[b] Xingmeng Lu,[e] Lian Yu,[e] Jianrong Li[a]

Department of Veterinary Biosciences, College of Veterinary Medicine, The Ohio State University, Columbus, Ohio, USA[a]; Food Animal Health Research Program, Ohio Agricultural Research and Development Center, Wooster, Ohio, USA[b]; Department of Pathology, College of Medicine, The Ohio State University, Columbus, Ohio, USA[c]; Southeast Poultry Research Laboratory, USDA Agricultural Research Service, Athens, Georgia, USA[d]; College of Animal Science, Zhejiang University, Hangzhou, Zhejiang, China[e]

ABSTRACT

Avian metapneumovirus (aMPV), also known as avian pneumovirus or turkey rhinotracheitis virus, is the causative agent of turkey rhinotracheitis and is associated with swollen head syndrome in chickens. Since its discovery in the 1970s, aMPV has been recognized as an economically important pathogen in the poultry industry worldwide. The conserved region VI (CR VI) of the large (L) polymerase proteins of paramyxoviruses catalyzes methyltransferase (MTase) activities that typically methylate viral mRNAs at guanine N-7 (G-N-7) and ribose 2′-O positions. In this study, we generated a panel of recombinant aMPV (raMPV) Colorado strains carrying mutations in the *S*-adenosyl methionine (SAM) binding site in the CR VI of L protein. These recombinant viruses were specifically defective in ribose 2′-O, but not G-N-7 methylation and were genetically stable and highly attenuated in cell culture and viral replication in the upper and lower respiratory tracts of specific-pathogen-free (SPF) young turkeys. Importantly, turkeys vaccinated with these MTase-defective raMPVs triggered a high level of neutralizing antibody and were completely protected from challenge with homologous aMPV Colorado strain and heterologous aMPV Minnesota strain. Collectively, our results indicate (i) that aMPV lacking 2′-O methylation is highly attenuated *in vitro* and *in vivo* and (ii) that inhibition of mRNA cap MTase can serve as a novel target to rationally design live attenuated vaccines for aMPV and perhaps other paramyxoviruses.

IMPORTANCE

Paramyxoviruses include many economically and agriculturally important viruses such as avian metapneumovirus (aMPV), and Newcastle disease virus (NDV), human pathogens such as human respiratory syncytial virus, human metapneumovirus, human parainfluenza virus type 3, and measles virus, and highly lethal emerging pathogens such as Nipah virus and Hendra virus. For many of them, there is no effective vaccine or antiviral drug. These viruses share common strategies for viral gene expression and replication. During transcription, paramyxoviruses produce capped, methylated, and polyadenylated mRNAs. Using aMPV as a model, we found that viral ribose 2′-*O* methyltransferase (MTase) is a novel approach to rationally attenuate the virus for vaccine purpose. Recombinant aMPV (raMPV) lacking 2′-*O* MTase were not only highly attenuated in turkeys but also provided complete protection against the challenge of homologous and heterologous aMPV strains. This novel approach can be applicable to other animal and human paramyxoviruses for rationally designing live attenuated vaccines.

Avian metapneumovirus (aMPV), also known as avian pneumovirus (APV) or turkey rhinotracheitis virus, is an economically important pathogen that causes an acute, highly contagious respiratory disease in turkeys and is the etiological agent of swollen-head syndrome in chickens (1–3). Since the first isolation of aMPV in South Africa in 1978, the virus has become prevalent worldwide (3, 4). Based on antigenicity and genetic diversity, four subtypes of aMPV, designated A, B, C, and D, have been characterized (1, 2, 4). Subtypes A, B, and D are found mainly in Europe and Asia (5–8). In the United States, aMPV was first identified in 1996, in a commercial turkey flock with respiratory diseases in Colorado (9). The virus was classified as subtype C due to its low sequence identity to subtype A and B viruses (6, 9). Subsequently, it emerged in turkey flocks in Minnesota and became a major problem in the turkey industry in the United States (10, 11). Epidemiological studies suggest that aMPV subtype C is distributed in a wide range of avian species, such as chickens, ducks, geese, American crows, cattle egrets, American coots, and pigeons (12, 13). A recent phylogenetic analysis showed that two distinct sublineages of aMPV subtype C exist in the United States (4). Clinical signs of aMPV in turkeys are characterized by coughing, sneezing, nasal discharge, and swollen infraorbital sinuses (3). Infected flocks have high morbidity (50 to 100%) at all ages, with mortality ranging from 0.5% in adult turkeys to 80% in young poults (1, 3). Direct economic losses caused by this virus include poor weight

Received 16 April 2014 **Accepted** 7 August 2014
Published ahead of print 13 August 2014
Editor: A. García-Sastre
Address correspondence to Jianrong Li, li.926@osu.edu.
J.S. and Y.W. contributed equally to this article.

doi:10.1128/JVI.01095-14

gain, sharply reduced egg production, poor egg quality, and high morbidity and mortality.

AMPV is a nonsegmented negative-sense (NNS) RNA virus, belonging to the genus *Metapneumovirus* in the subfamily *Pneumovirinae* of the family *Paramyxoviridae*. The only other member in the genus *Metapneumovirus* is the human metapneumovirus (hMPV), which was first identified in infants and children with acute respiratory tract infections in 2001 in the Netherlands (14). Soon after its discovery, hMPV was recognized as a globally prevalent pathogen and a major causative agent of acute respiratory tract disease in individuals of all ages, especially infants, children, the elderly, and immunocompromised individuals (15). Interestingly, aMPV subtype C shares more homology with hMPV than the other three aMPV subtypes (15, 16). In addition, turkeys were shown to be susceptible to hMPV infection (17). Paramyxoviruses include many other important human pathogens, such as human respiratory syncytial virus (RSV), human parainfluenza virus type 3 (PIV3), measles virus, and mump virus, highly lethal emerging pathogens such as Nipah virus and Hendra virus, and agriculturally important viruses such as Newcastle disease virus (NDV). For many of these viruses, there are no effective vaccines or antiviral drugs.

Since the discovery of aMPV, many attempts have been made to develop a vaccine for this virus. In Europe, live attenuated vaccines have been developed by blind passage of the virulent strains in tissue culture, and these have been used for the prevention of aMPV type A and B viruses (3, 18). After the emergence of aMPV in the United States, a subtype C strain, aMPV/MN-1a, was attenuated through 63 serial passages of the virus in cell culture (19). This strain triggered a considerable level of antibody response and protected poults from the virulent challenge (19). In addition, cold-adapted aMPV was also shown to be a good vaccine candidate (20). Despite the vaccination of commercial turkeys, outbreaks of aMPV still occur worldwide (3, 21, 22). In addition, it was reported that a live aMPV vaccine reverted to a virulent strain and became persistent in the field (22, 23). Therefore, there is an urgent need to develop a more stable and efficacious vaccine for aMPV.

The large (L) polymerase protein of NNS RNA viruses is a multifunctional protein that possesses all of the enzymatic activities for genome replication, mRNA synthesis, and mRNA modifications including capping, methylation, and polyadenylation (reviewed in reference 24). Using vesicular stomatitis virus (VSV), a prototypical NNS RNA virus, as a model, these enzymatic activities have been mapped to the amino acid level in L protein. For example, a GDN motif in conserved region (CR) III of the L protein was found to be essential for nucleotide polymerization (24, 25). An unconventional mRNA capping enzyme, the polyribonucelotidyltransferase (PRNTase) activity, has been mapped to the HR motif within CR V of the L protein (26, 27). An unusual dual methyltransferase (MTase) that methylates virus-specific mRNAs at the positions guanine N-7 (G-N-7) and ribose-2′-O (2′-O) has been identified in the CR VI of the L protein (28, 29). These signature motifs are conserved in all members in *Rhabdoviridae*, *Paramyxoviridae*, and *Filoviridae*. These breakthroughs revealed that mRNA cap formation is a novel and universal target for drug discovery and vaccine development for all NNS RNA viruses. For instance, small molecules that inhibit mRNA capping would likely be lethal to virus. On the other hand, inhibition of mRNA cap methylation may yield attenuated strains that can be used for the development of live vaccine candidates. In fact, the concept of using mRNA cap methylation as a target for virus attenuation has been recently proved in VSV (30). Specifically, we found that recombinant VSV (rVSV) mutants rVSV-K1651A, -D1762A, and -E1833Q, which are defective in both G-N-7 and 2′O methylation, were highly attenuated in mice. The rVSV-G1670A and -G1672A viruses, which are defective in G-N-7 but not 2′-O methylation, retained low virulence in mice.

In this study, we employed this novel attenuation strategy on aMPV, an economically important avian pathogen. We found that mutations to the binding site for the methyl donor, *S*-adenosyl methionine (SAM), yielded a panel of recombinant aMPVs (raMPVs) that were highly attenuated in viral replication in the upper and lower respiratory tract of turkeys. Unlike VSV carrying mutations in the SAM binding site, these raMPV mutants were specifically defective in 2′-O, but not G-N-7, methylation. Importantly, turkeys vaccinated with these 2′-O methylation-defective raMPVs generated a high level of antibody that provided complete protection against the homologous aMPV Colorado strain and the heterologous aMPV Minnesota strain. Therefore, 2′-O methylation-defective raMPVs are excellent live vaccine candidates.

MATERIALS AND METHODS

Cell lines. Vero E6 cells (ATCC CRL-1586) and BHK-SR19-T7 cells (kindly provided by Apath, L.L.C, Brooklyn, NY) were grown in Dulbecco's modified Eagle's medium (DMEM; Life Technologies, Bethesda, MD) supplemented with 10% fetal bovine serum (FBS). The medium of the BHK-SR19-T7 cells was supplemented with 10 μg/ml puromycin (Life Technologies) during every other passage to select for T7 polymerase-expressing cells. LLC-MK2 (ATCC CCL-7) cells were maintained in Opti-MEM (Life Technologies) supplemented with 2% FBS.

Virus stock. aMPV subtype C Colorado strain (aMPV/Colorado/turkey/96 [aMPV-CO]) was obtained from the pathogen repository bank at the Southeast Poultry Research Laboratory (SEPRL; USDA-ARS, Athens, GA, USA) (31). aMPV subtype C Minnesota strain (aMPV/Minnesota/turkey/2a/97 [aMPV-MN]) was provided by the Ohio Agricultural Research and Development Center, Wooster, OH (1). aMPV-CO and aMPV-MN were originally isolated from turkey flocks in Colorado and Minnesota, respectively. Both strains were virulent in turkeys and were grown in Vero-E6 cells as previously described (1, 31). Wild-type rVSV and mutants (rVSV-K1651A and -G1670A) were provided by Sean Whelan at Harvard Medical School. Recombinant rVSV-K1651A lacks both G-N-7 and 2′-O methylation, whereas rVSV-G1670A is specifically defective in G-N-7 but not 2′-O methylation (28, 29).

Plasmids and site-directed mutagenesis. Plasmids encoding the aMPV minigenome and the full-length anti-genomic cDNA of aMPV-CO and support plasmids expressing aMPV N (pCDNA3-N), P (pCDNA3-P), L (pCDNA3-L), and M2-1 (pCDNA3-M2-1) proteins were generated previously (31). The L CR VI mutations were introduced into the full-length genome of the wild-type aMPV-CO strain. A QuikChange site-directed mutagenesis kit (Strategene, La Jolla, CA) was utilized according to the manufacturer's recommendations. Mutations were confirmed by DNA sequencing.

Recovery of recombinant aMPVs from the full-length cDNA clones. Recombinant aMPVs (raMPVs) were rescued using a reverse-genetics system as described previously (31). Briefly, BHK-SR19-T7 cells (kindly provided by Apath, L.L.C.) were transfected with 5.0 μg of paMPV full-length genomic plasmid, 2.0 μg of pCDNA3-N, 2.0 μg of pCDNA3-P, 1.0 μg of pCDNA3-L, and 1.0 μg of pCDNA3-M2-1 using Lipofectamine 2000 (Life Technologies). At day 4 posttransfection, the cells were harvested using scrapers and cocultured with 50 to 60% confluent Vero-E6 cells. When an extensive cytopathic effect (CPE) was observed, the cells were subjected to three freeze-thaw cycles, followed by centrifugation at

3,000 × *g* for 10 min. The supernatant was used subsequently to infect new Vero-E6 cells. The successful recovery of the raMPVs was confirmed by agarose overlay plaque assay and reverse transcription-PCR (RT-PCR).

Purification of aMPV. The raMPV stocks used in animal studies were grown in Vero-E6 cells and purified by ultracentrifugation. Briefly, Vero-E6 cells in 10 confluent T150 flasks were infected with each raMPV at a multiplicity of infection (MOI) of 0.1 in a volume of 2 ml of DMEM. After 1 h of adsorption with constant shaking, 20 ml of Opti-MEM (supplemented with 2% FBS) was added to the cultures, and infected cells were incubated at 37°C for 4 days. When extensive CPE was observed, cells were harvested by scraping. The cell suspension was clarified by low-speed centrifugation at 3,000 × *g* for 20 min at 4°C in a Beckman Coulter Allegra 6R centrifuge. The cell pellet was resuspended in 2 ml of Opti-MEM and subjected to three freeze-thaw cycles. The mixture was clarified by low-speed centrifugation, and the supernatants were combined. The virus was pelleted by ultracentrifugation at 28,000 × *g* in a Beckman Ty 50.2 rotor for 2 h. The final virus pellet was resuspended in 0.3 ml of Opti-MEM, aliquoted, and stored at −80°C in a freezer. One vial of virus was thawed, and the titer was determined by plaque assay or $TCID_{50}$.

Viral replication kinetics in Vero-E6 cells. Confluent Vero-E6 cells in 35-mm dishes were infected by raMPV or mutant raMPV at an MOI of 0.1. After 1 h of adsorption, the inoculum was removed, and cells were washed three times with phosphate-buffered saline (PBS). Fresh DMEM (supplemented with 2% FBS) was added, and the infected cells were incubated at 37°C. At different time points postinfection, the supernatant and cells were harvested by three freeze-thaw cycles, followed by centrifugation at 1,500 × *g* at room temperature (RT) for 15 min. Virus titer was determined by plaque assay in Vero-E6 cells.

$TCID_{50}$ assay. Vero-E6 cells were seeded in 96-well plates (Corning, Lowell, MA) at a density of 10^5 cells per well and were grown at 37°C for 18 h. Upon infection, the medium was removed, and 0.2 ml of 10-fold serial virus dilutions in Opti-MEM was added to each well. Eight wells containing a monolayer of cells were infected with 50 μl of each virus dilution, and the CPE was examined under a microscope daily for 10 days postinfection. The CPE was recorded, and the virus titer was calculated as the 50% tissue culture infective dose ($TCID_{50}$) using the Reed-Muench method (32).

aMPV plaque assay. An aMPV plaque assay was performed using a procedure described previously (33). Vero cells were seeded in six-well plates at a density of 2×10^6 cells per well. After incubation for 18 h, the medium was removed, and cell monolayers were infected with 400 μl of a 10-fold dilution series of each virus. After incubation at 37°C for 1 h with agitation every 10 min, the cells in each well were overlaid with 2.5 ml of Eagle's minimum essential medium (MEM) containing 1% agarose, 1% FBS, 0.075% sodium bicarbonate ($NaHCO_3$), 20 mM HEPES (pH 7.7), 2 mM L-glutamine, 12.5 mg/ml of penicillin, 4 mg/ml of streptomycin, and 4 mg/ml of kanamycin. The overlay medium was supplemented with actinomycin-D (Sigma, Louis, MO) (0.2 μg/ml) and tosylsulfonyl phenylalanyl chloromethyl ketone (TPCK)-trypsin (0.1 to 0.6 μg/ml). The plates were incubated at 4°C for 30 min to solidify the overlay medium. Cells were then grown at 37°C and 5% CO_2 to allow for plaque formation. After incubation for 7 days, the cells were fixed in 10% (vol/vol) formaldehyde for 2 h, and the plaques were visualized by staining with 0.05% (wt/vol) crystal violet.

Genetic stability of raMPV mutants in cell culture. Confluent Vero-E6 cells in T25 flasks were infected by each mutant raMPV at an MOI of 0.1. When extensive CPE was observed, the cell culture supernatant was harvested and used for the next passage in Vero-E6 cells. Each raMPV mutant was repeatedly passaged 12 times in Vero-E6 cells. At each passage, the CR VI of the L gene was amplified by RT-PCR and sequenced. At passage 12, the entire genome of each recombinant virus was amplified by RT-PCR and sequenced.

***In vitro trans*-methylation assay.** An *in vitro trans*-methylation assay was performed using a method reported by Zust et al. with some modifications (34). Briefly, confluent Vero-E6 cells in 150-mm dishes were mock infected or infected by raMPV mutants or rVSV mutants at an MOI of 0.1 in the presence of actinomycin D (0.6 μg/ml). When extensive CPE was observed, total RNA was isolated from virus-infected cells using TRIzol reagent (Life Technologies) and dissolved in 10 mM Tris-HCl buffer (pH 7.5). Subsequently, poly(A)-containing RNA was isolated from total RNA using a Dynabeads mRNA isolation kit (Life Technologies) according to the manufacturer's recommendations. Subsequently, hMPV-specific mRNA (N mRNA) and cellular mRNA (glyceraldehyde-3-phosphate dehydrogenase [GAPDH] mRNA) were quantified by real-time RT-PCR. To determine whether raMPV or rVSV mutants were defective in G-N-7 methylation, 500 ng of mRNA (based on the quantification of GAPDH RNAs) was incubated with 10 units of vaccinia virus G-N-7 MTase supplied by an m^7G capping system (Cellscript, Madison, WI) in the presence of 15 μCi of [^{3}H]SAM (85 Ci/mmol; PerkinElmer, Wellesley, MA) for 4 h. After the methylation reaction, RNA was purified using an RNeasy mini-kit (Qiagen, Valencia, CA), and the methylation of the mRNA cap structure was measured by ^{3}H incorporation using a 1414 series scintillation counter (PerkinElmer). The ^{3}H incorporation (in corrected counts per minute [ccpm]) from wild-type and mutant aMPV samples was reduced by the ccpm of RNA from mock-infected cells. Finally, the ccpm was normalized by virus-specific mRNA. Similarly, a *trans*-ribose 2′-O methylation assay was performed using mRNA purified from raMPV mutant-infected or rVSV mutant-infected cells. Briefly, 500 ng of mRNAs was incubated with 10 units of vaccinia virus 2′-*O* MTase supplied by a vaccinia 2′-*O*-methyltransferase kit (Cellscript) in the presence of 15 μCi of [^{3}H]SAM (85 Ci/mmol; PerkinElmer). After the methylation reaction, RNA was purified, and the level of 2′-O methylation was measured by ^{3}H incorporation using a scintillation counter. The ccpm was normalized by virus-specific mRNA. The ratio of [^{3}H]SAM incorporation between each mutant and wild-type virus was calculated.

Animal experiment 1: replication and pathogenesis of raMPV and mutants in turkey poults. Specific-pathogen-free (SPF) turkey poults were used in these studies. The animal study was conducted in strict accordance with USDA regulations and the recommendations in the Guide for the Care and Use of Laboratory Animals of the National Institutes of Health and was approved by The Ohio State University Institutional Animal Care and Use Committee (animal protocol no. 2012A00000078). Turkeys were housed in cages inside high-security isolation rooms provided with HEPA-filtered intake and exhaust air at The Ohio Agriculture Research and Development Center, The Ohio State University. The animal care facilities at The Ohio State University are AAALAC accredited. Prior to the animal study, blood samples were collected from each turkey to confirm that it was negative for aMPV antibody. Seventy-two 2-week-old poults were randomly allotted into six groups (12 poults per group). Each inoculated group was separately housed in cages under biosafety level 2 (BSL-2) conditions. Turkey poults in group 1 were inoculated with 200 μl of DMEM containing 2.0×10^5 $TCID_{50}$ of raMPV and served as a positive control. Poults in groups 2 to 6 were inoculated with 200 μl of DMEM containing 2.0×10^5 $TCID_{50}$ of each of four raMPV mutants (raMPV-G1696A, -D1700A, -N1701A, and -D1755A). Poults in group 7 were mock infected with 200 μl of DMEM and served as uninfected controls. All virus inoculation was done via the oculonasal route. After inoculation, the animals were observed daily for mortality and morbidity. At 3, 5, 7, and 10 days postinoculation (dpi), three turkeys from each group were euthanized. Sinus and trachea swabs were collected and eluted in 1 ml of DMEM for virus and viral RNA detection. Lungs and tracheas were collected for virus isolation, viral RNA detection, and histological analysis.

Animal experiment 2: protection efficacy against challenge with homologous aMPV-CO strain. A total of 105 2-week-old SPF turkey poults were randomly divided to seven groups (15 turkeys per group). Turkeys in group 1 were inoculated with DMEM and served as the unimmunized but challenged positive controls. Turkey poults in groups 2 to 6 were vaccinated intranasally with 2×10^5 $TCID_{50}$ of raMPV-CO or mutants (raMPV-G1696A, -G1700A, -N1701A, and -D1755A). Turkeys in group 7 were inoculated with DMEM and served as the uninfected control (neg-

ative control). After vaccination, the animals were observed for mortality and morbidity. Blood samples were collected from each turkey at week 3 postimmunization, and serum was separated for antibody detection. At week 3 postimmunization, turkeys in groups 1 to 6 were challenged with raMPV-CO at a dose of 1.0×10^6 $TCID_{50}$ per turkey. All virus challenge was done via the oculonasal route. After challenge, the animals were observed every day for mortality and morbidity associated with aMPV infection. At 3, 5, and 7 days postchallenge (dpc), 5 turkey poults from each group were euthanized. Sinus and trachea swabs were collected and eluted in 1 ml of DMEM for virus and viral RNA detection. Lungs and trachea were collected for virus isolation, viral RNA detection, and histological analysis. The immunogenicity of the MTase-defective aMPVs was evaluated using the following methods. (i) Humoral immunity was determined by a virus-serum neutralization assay using an endpoint dilution plaque reduction assay. (ii) Viral titer in the sinus and trachea swabs and in lungs was determined by plaque assay or $TCID_{50}$ assay, and viral genomic RNA was quantified by real-time RT-PCR. (iii) Tracheal and pulmonary histology were evaluated. The protection was evaluated based on clinical signs, viral replication, and tracheal and pulmonary histology.

Animal experiment 3: protection efficacy against challenge with heterologous aMPV-MN strain. A total of 105 2-week-old SPF turkey poults were randomly divided to seven groups (15 turkeys per group). The experimental design and procedure were identical to those described for animal experiment 2 except that the challenge virus was changed to aMPV-MN.

Histology. After euthanization, the trachea and right lung of each bird were removed, inflated, and fixed in 4% neutral buffered formaldehyde. Fixed tissues were embedded in paraffin and sectioned at 5 μm. Slides were then stained with hematoxylin and eosin (H&E) for the examination of histological changes by light microscopy.

Determination of aMPV neutralizing antibody. aMPV-specific neutralizing antibody titers were determined using a plaque reduction neutralizing assay (35). The serum samples from turkeys were heat inactivated at 56°C for 30 min. Two-fold dilutions of serum samples were mixed with an equal volume of DMEM containing approximately 100 PFU/well aMPV-CO in a 96-well plate and incubated at room temperature for 1 h with constant rotation. The mixtures were then transferred to confluent Vero-E6 cells in a 96-well plate in triplicate. After 1 h of incubation at 37°C, the virus-serum mixtures were removed, and the cells were overlaid with 0.75% methylcellulose in DMEM and incubated for another 4 days before virus plaque titration as described previously. Plaques were counted, and 50% plaque reduction titers were calculated as aMPV-specific neutralizing antibody titers.

Determination of viral titer in sinus, trachea, and lung samples. Sinus and trachea swabs were collected from all the turkey experiments. The swabs were eluted in 1 ml of DMEM by vortexing for 1 min. After centrifugation at 3,000 × *g* for 10 min, the supernatants were collected for virus detection. After euthanization, in each animal experiment the left lung from each turkey poult was removed, weighed, and homogenized in 5 ml of phosphate-buffered saline (PBS) solution using a Precellys 24 tissue homogenizer (Bertin Corp., MD) according to the manufacturer's recommendations. The presence of infectious virus was determined by $TCID_{50}$ assay in Vero-E6 cells as described above.

RT-PCR and sequencing. All plasmids, virus stocks, and virus isolates from sinus, trachea, and lungs of turkeys were sequenced. Viral RNA was extracted from 200 μl of each recombinant virus using an RNeasy minikit (Qiagen) according to the manufacturer's recommendation. A 520-bp DNA fragment spanning CR VI of the aMPV L gene was amplified by RT-PCR using the following primers, designed to anneal to nucleotide positions 12938 and 13464 (numbers are based on the genome sequence of aMPV-CO), respectively: aMPV-L-12938-Forward: 5′-CAGCTCTAC CGGTTGCAAAATAAGTGTCAAAGCATGT-3′ and aMPV-L-13464-Reverse: 5′-TAGAAGGACATAACACTCGGATCCTGACAGTTT-3′.

The PCR products were purified and sequenced at The Ohio State University Plant Microbe Genetics Facility to confirm the presence of the designed mutations. Since the initial recovered virus stocks might contain original plasmid DNA, the stocks were digested with DNase I (Invitrogen), followed by RNA extraction and RT-PCR. In addition, PCR alone (without the RT step) was performed to confirm the complete digestion of plasmid DNA.

Quantification of viral genomic RNA by real-time RT-PCR. Total RNA was extracted from sinus and tracheal swabs and from lungs by a Qiagen RNeasy minikit (Qiagen) according to the manufacturer's recommendation. A total of 200 μl of homogenized lung tissue samples and 150 μl of sinus and tracheal swab fluids were used for viral RNA extraction. Viral genomic RNA copies (GRC) from each sample were quantitated by real-time RT-PCR using SYBR green master mix (Applied Biosystems). The PCR conditions and cycles were as follows: initial DNA denaturation for 10 min at 95°C, followed by 45 cycles at 95°C for 10 s, followed by an annealing step at 58°C for 10 s, extension at 72°C for 10 s, and then signal detection 81°C for 2 s. A plasmid containing the full-length genome of aMPV-CO was used as a standard. Viral RNA level in lungs was expressed as log GRC/g. Viral RNA level in sinus and tracheal swab fluid was expressed as log GRC/ml.

Statistical analysis. Statistical analysis was performed by one-way multiple comparisons using SPSS, version 8.0, statistical analysis software (SPSS Inc., Chicago, IL). A P value of <0.05 was considered statistically significant.

RESULTS

Mutagenesis analysis in the predicted SAM binding site in aMPV L protein. The SAM-dependent MTase superfamily contains a series of conserved motifs including a G-rich motif and an acidic residue (D/E) that are involved in binding SAM, the methyl donor (36, 37). Sequence alignments showed that this binding site is conserved in L proteins of all NNS RNA viruses with the exception of Bona disease virus (Fig. 1). In VSV L protein, these amino acids include G1670, G1672, G1674, G1675, and D1735. Previously, we showed that rVSV-G1670A and -G1672A were specifically defective in G-N-7 but not 2′-O methylation, whereas rVSV-G1675A abolished both G-N-7 and 2′-O methylations (29). In addition, rVSV-D1735A diminished both G-N-7 and 2′-O methylation by approximately 70% (29). In contrast, rVSV-G1674A did not significantly impact G-N-7 or 2′-O methylation, but it was sensitive to SAM concentration (28, 29). The equivalent amino acids in aMPV L protein include G1696, G1698, G1700, N1701, and D1755 (Fig. 1). Thus, each of these amino acid residues was changed to alanine in aMPV L.

Recovery of recombinant aMPV (raMPV) with mutations in the SAM binding site. The amino acids in the predicted SAM binding motif were individually mutated to alanines in the full-length genomic cDNA of the aMPV subtype C CO strain. Using a reverse-genetics system, we recovered four recombinant viruses, raMPV-G1696A, -G1700A, -N1701A, and -D1755A. However, we failed to recover the G1698A mutant in multiple attempts. As shown in Fig. 2, all raMPV mutants showed significantly smaller plaque sizes than the raMPV plaque size in a direct agarose overlay plaque assay. After 7 days of incubation, the plaque sizes of raMPV-G1696A, -G1700A, -N1701A, and -D1755A were 0.92 ± 0.34 mm, 1.12 ± 0.24 mm, 0.82 ± 0.31 mm, and 0.51 ± 0.20 mm, respectively. In contrast, the plaque size of raMPV was 2.25 ± 0.35 mm. Thus, these mutant viruses showed defects in cell-cell spread and/or viral growth, as judged by their plaque morphology. To confirm that the mutant raMPVs contained the desired mutations, virus stocks were treated with DNase I to remove the possible contamination of plasmid DNA from transfection, followed by RNA extraction. The CR VI of the L gene of each virus was ampli-

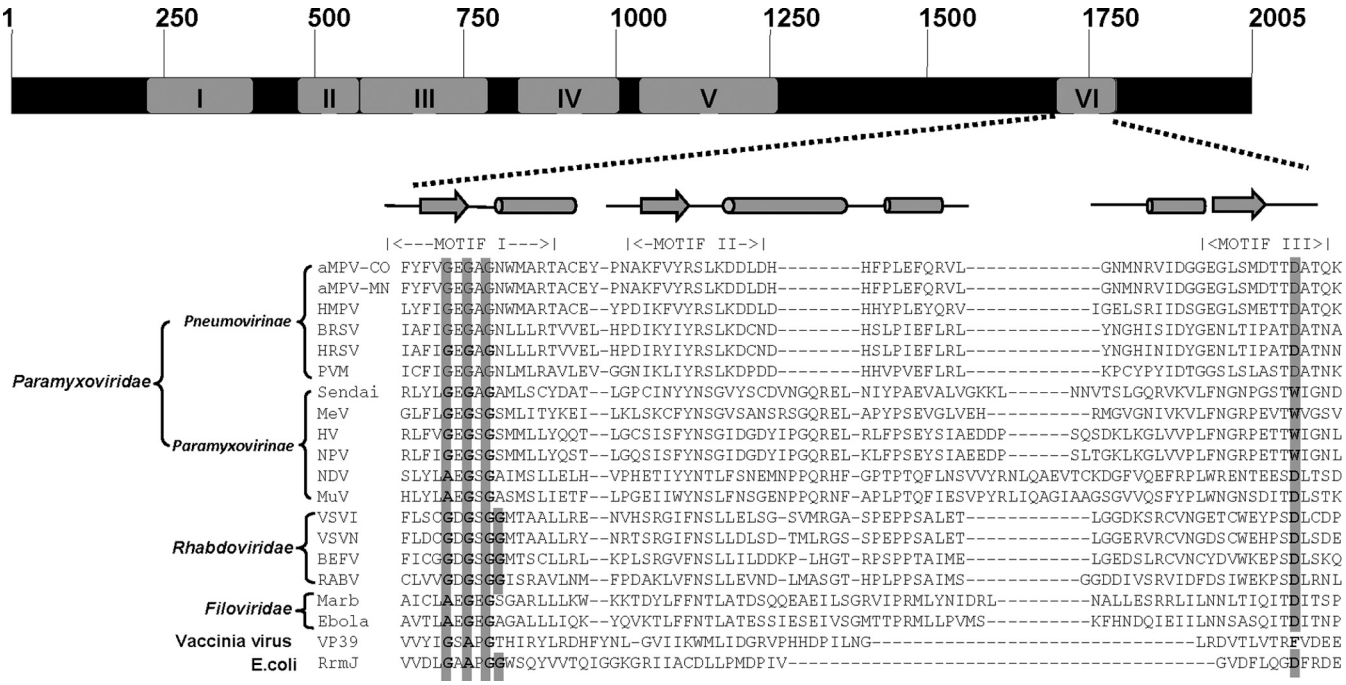

FIG 1 Sequence alignment of SAM binding site in conserved domain VI of L proteins of NNS RNA viruses. A schematic of the conserved regions (CR) in the L proteins is shown at the top of the figure. Amino acid sequence alignment identified six CRs, numbered I to VI in L proteins. The functions of CRs III, V, and VI have been mapped in VSV L protein. Predicted or known alpha-helical regions are shown as cylinders, and the β-sheet regions are shown as arrows. Below the schematic, the sequence alignment of SAM binding sites is shown for representative viruses. *Escherichia coli* RRMJ and vaccinia virus VP39 are shown for comparison. The predicted SAM binding site (GXGXG . . . D) is shown by gray boxes. Representative members of the *Pneumovirinae* (aMPV-CO, avian metapneumovirus Colorado strain; aMPV-MN, avian metapneumovirus Minnesota strain; HMPV, human metapneumovirus; HRSV, human respiratory syncytial virus; BRSV, bovine respiratory syncytial virus; PVM, pneumonia virus of mice), *Paramyxovirinae* (MeV, Measles virus; HV, Hendra virus; NPV, Nipah virus; MuV, Mump; NDV, Newcastle disease virus), *Filoviridae* (EBOM, Ebola virus; Marb, Marburg virus), and *Rhabdoviridae* (VSVI, vesicular stomatitis virus Indiana serotype; VSVI, vesicular stomatitis virus New Jersey serotype; BEFV, bovine ephemeral fever virus; RABV, Rabies virus) are shown.

fied by RT-PCR, and sequence analysis confirmed the presence of the mutation in all raMPV mutants (data not shown). Finally, the entire genomes of these recombinants were sequenced to confirm that no additional mutation(s) had been introduced (data not shown).

Recombinant aMPVs carrying mutations in the SAM binding site had a delay in viral replication. The replication kinetics of raMPV mutants in Vero-E6 cells was determined. As shown in Fig. 3, all raMPV mutants had a 1- to 2-day delay in viral growth compared to raMPV. The time for reaching peak titer for these mutants ranged from 4 to 5 days postinfection, whereas raMPV reached a peak titer at day 3 postinfection. Interestingly, raMPV-G1700A replicated to a higher titer than wild-type raMPV ($P < 0.05$) even though it had a 2-day delay in replication. The peak titer of raMPV-G1700A was 7.24 $\log_{10}$ PFU/ml, which was 1.1 logs higher than that of raMPV (6.10 $\log_{10}$ PFU/ml) ($P < 0.05$). The peak titers of raMPV-N1701A and raMPV-G1696A were 6.16 and 5.70 $\log_{10}$ PFU/ml, respectively, values which were similar to the raMPV titer ($P > 0.05$). There was no significant difference in replication kinetics between raMPV-N1701A and raMPV ($P > 0.05$). The peak titer of raMPV-D1755A was 5.27 $\log_{10}$ PFU/ml, which was only approximately 0.8 log less than that of raMPV ($P < 0.05$). The cytopathic effect (CPE) of these recombinant viruses in Vero cells is shown in Fig. 4. Wild-type raMPV-CO induced obvious CPE at day 2 postinoculation. The CPE caused by the raMPV mutants was significantly delayed. Therefore, raMPVs carrying mutations in the SAM binding site had delays in viral replication and were attenuated in cell culture.

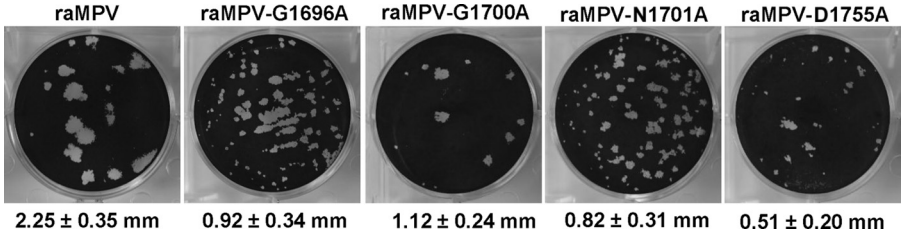

FIG 2 Plaque morphology of recombinant aMPVs carrying mutations in the SAM binding site. An agarose overlay plaque assay was performed in monolayer Vero-E6 cells. Viral plaques were developed at day 7 postinfection. The cells were fixed in 10% formaldehyde, and the plaques were visualized by staining with crystal violet.

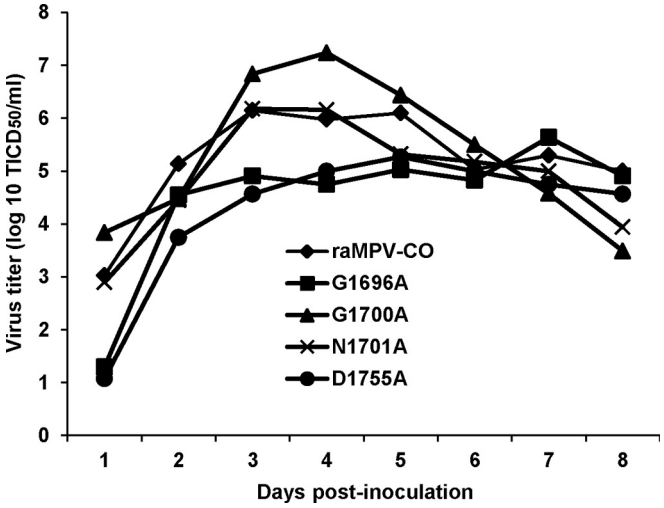

FIG 3 Multistep growth curve of recombinant hMPVs carrying mutations in the SAM binding site. Vero-E6 cells in 35-mm dishes were infected with each recombinant raMPV at an MOI of 0.1. After adsorption for 1 h, the inocula were removed, and the infected cells were washed three times with Opti-MEM. Then, fresh Opti-MEM containing 2% FBS was added, and cells were incubated at 37°C for various time periods. Aliquots of the cell culture fluid were removed at the indicated intervals. Viral titer was determined by $TCID_{50}$ assay in Vero-E6 cells.

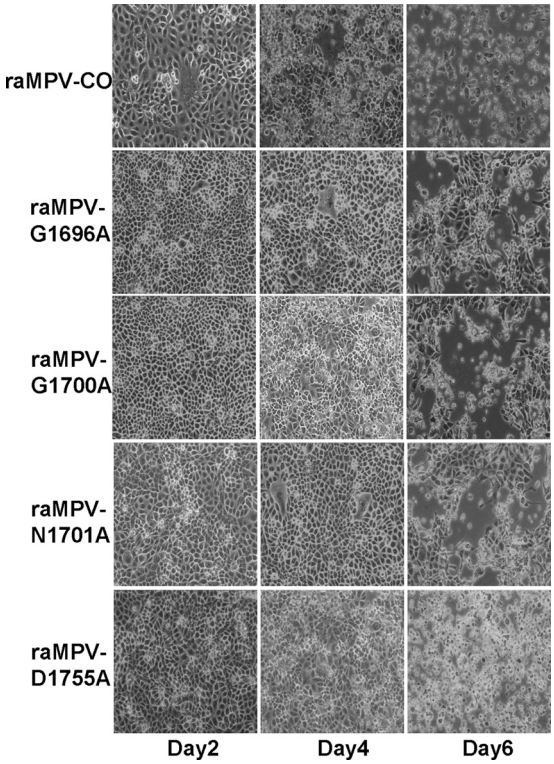

FIG 4 Cytopathic effects (CPEs) caused by raMPVs carrying mutations in the SAM binding site. Vero-E6 cells were infected with each recombinant aMPV at an MOI of 0.1. CPE was monitored on a daily basis. Pictures were taken at days 2, 4, and 6 postinfection.

Genetic stability of raMPV mutants in cell culture. The genetic stability of each raMPV mutant was determined by passaging virus 12 times in Vero-E6 cells. The CR VI of the L gene from each passage was sequenced. Results showed that all raMPV mutants retained their mutation in the CR VI of the L gene. At passage 12, the entire genome of each recombinant virus was sequenced. Except for the desired mutation in the MTase region in the L gene, no mutations were found in the genome after 12 passages. This result suggests that these raMPV mutants are genetically stable.

Recombinant aMPV carrying mutations in the SAM binding site are defective in 2′-O but not G-N-7 methylation. In the last several decades, VSV has been used as a model to study mRNA processing in NNS RNA viruses because it has a robust *in vitro* RNA reconstitution assay that allows analysis of mRNA capping, methylation, and polyadenylation (24). Using this assay, we showed that rVSV carrying a point mutation in the SAM binding site (rVSV-G1670A) specifically abolished G-N-7 but not 2′-O methylation (29). In contrast, rVSV carrying a point mutation in the MTase catalytic site (rVSV-K1651A) abolished both G-N-7 and 2′-O methylations (28). Unlike VSV, most paramyxoviruses, including aMPV, are unable to synthesize mRNA *in vitro* using purified virus particles. We have developed a *trans*-methylation assay that allows us to analyze cap methylation of viral mRNA in virus-infected cells. In this experiment, we used rVSV, rVSV-K1651A, and rVSV-G1670A as controls since their status with respect to mRNA cap methylation has been well defined. Briefly, Vero-E6 cells were mock infected or infected by raMPV mutants or rVSV mutants at an MOI of 0.1, and mRNAs for each recombinant virus were harvested. To determine whether these viral mutants were defective in G-N-7 methylation, equal amounts of mRNA from each mutant was incubated with 10 units of vaccinia virus G-N-7 MTase in the presence of 15 μCi of [^{3}H]SAM. After the methylation reaction, RNA was purified, and the methylation of the mRNA cap structure was quantified by determining the ^{3}H incorporation with a scintillation counter. The [^{3}H]SAM incorporation (ccpm) from wild-type or mutant virus was reduced by the ccpm of RNA from mock-infected cells (background control). The ccpm was normalized by virus-specific mRNA. In addition, the ratio of ^{3}H incorporation between the raMPV mutant and raMPV was calculated. As shown in Fig. 5A, raMPV mRNAs were not methylated by vaccinia virus G-N-7 MTase, which is consistent with this site already being methylated by the raMPV enzymes. Similarly, the [^{3}H]SAM incorporation of mRNAs produced by raMPV-G1696A, -G1700A, -N1701A, and -D1755A was indistinguishable from that of raMPV ($P > 0.05$), suggesting that mRNAs of these mutants already contain G-N-7 methylation and thus were not methylated by the exogenous vaccinia virus G-N-7 MTase. As shown in Fig. 5A, rVSV mRNAs were not methylated by vaccinia virus G-N-7 MTase, which is consistent with the fact that rVSV produces fully G-N-7-methylated mRNA. In contrast, mRNAs of rVSV-K1651A and -G1670A were efficiently methylated by vaccinia virus G-N-7 MTase. The ^{3}H incorporation of rVSV-K1651A and -G1670A was approximately 6.41- and 5.68-fold higher than that of wild-type rVSV, respectively. This is essentially consistent with our previous observation showing that rVSV-K1651A and -G1670A lacked G-N-7 methylation using an *in vitro* mRNA synthesis assay (28, 29). Therefore, this result indicates that rhMPV-G1696A, -G1700A, -N1701A, and -D1755A are not defective in G-N-7 methylation.

Similarly, we developed a *trans*-methylation assay to analyze 2′-O methylation of mRNAs isolated from virus-infected cells.

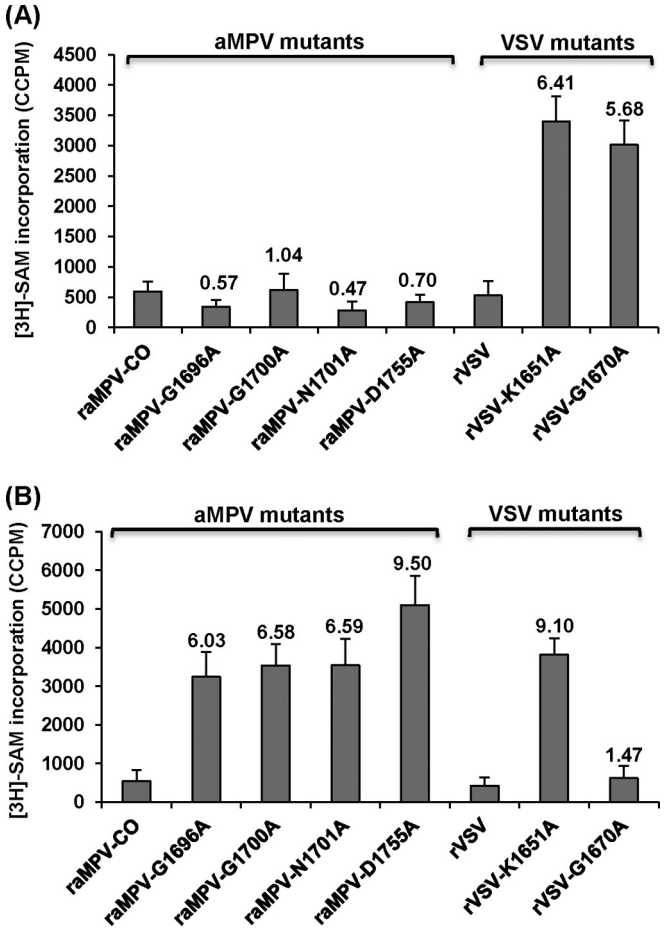

FIG 5 Analysis of aMPV mRNA cap methylation by *in vitro trans*-methylation assay. (A) G-N-7 *trans*-methylation assay. A total of 500 ng of mRNAs was isolated from aMPV- or VSV-infected cells and *trans*-methylated by vaccinia virus G-N-7 MTase in the presence of 15 μCi of [^{3}H]SAM as described in Materials and Methods. [^{3}H]SAM incorporation (ccpm) from wild-type or mutant aMPV was reduced by the ccpm of RNA from mock-infected cells. The ccpm was normalized by virus-specific mRNA. The number on the top of each column indicates the ratio of [^{3}H]SAM incorporation of viral mRNAs between mutant and wild-type viruses. The data are the average of three independent experiments. (B) 2′-O *trans*-methylation assay. A total of 500 ng of mRNAs was isolated from aMPV- or VSV-infected cells and premethylated by vaccinia virus G-N-7 MTase in the presence of 1 mM cold SAM. The RNAs were purified and further *trans*-methylated by vaccinia virus 2′-*O* MTase in the presence of 15 μCi o [^{3}H]SAM. The ccpm of [^{3}H]SAM incorporation for each virus is shown. The number on the top of each column indicates the ratio of [^{3}H]SAM incorporation of viral mRNAs between mutant and wild-type viruses. Data are the average of three independent experiments.

Briefly, equals amount of mRNAs of raMPV and rVSV mutants were incubated with 10 units of vaccinia virus 2′-*O* MTase (VP39) in the presence of 15 μCi of [^{3}H]SAM. After the methylation reaction, RNA was purified, and the level of 2′-O methylation was measured by ^{3}H incorporation using a scintillation counter. As shown in Fig. 5B, raMPV mRNAs were not methylated by vaccinia virus 2′-*O* MTase, suggesting that raMPV produces 2′-O-methylated mRNA. The ^{3}H incorporation of raMPV-G1696A, -G1700A, -N1701A, and -D1755A was 6.0- to 9.5-fold higher than that of wild-type raMPV-CO ($P < 0.05$), suggesting that these raMPV mutants had defects in 2′-O methylation. Again, VSV mutants were used as controls in this experiment. As shown in Fig. 5B, rVSV mRNAs were not methylated by vaccinia virus 2′-*O* MTase, which is consistent with the fact that rVSV produces fully 2′-O-methylated mRNAs. In contrast, mRNAs of rVSV-K1651A were efficiently methylated by vaccinia virus 2′-*O* MTase, demonstrating that rVSV-K1651A is defective in 2′-O methylation. The ^{3}H incorporation of rVSV-K1651A was approximately 9.1-fold higher than that of wild-type rVSV. However, ^{3}H incorporation of mRNAs produced by rVSV-G1670A was not significantly different from that of rVSV, demonstrating that rVSV-G1670A is not defective in 2′-O methylation. Collectively, two major conclusions can be drawn from the above-described experiments. First, for VSV mutants, the results of the *trans*-methylation assay using exogenous vaccinia G-N-7 and 2′-*O* MTases were essentially similar to those from an *in vitro* mRNA synthesis assay using purified VSV particles. Second, raMPVs carrying mutations in the SAM binding site were specifically defective in 2′-O, but not G-N-7, methylation.

Recombinant aMPV carrying mutations in the SAM binding site are attenuated in turkeys. The replication and pathogenesis of raMPV mutants were determined in turkey poults, the natural hosts of aMPV. Briefly, 2-week-old SPF turkeys were inoculated with 2×10^5 $TCID_{50}$s of raMPV-CO or raMPV mutants via the oculonasal route. After virus inoculation, clinical signs associated with aMPV infection were monitored daily. Three turkey poults from each group were euthanized at 3, 5, 7, and 10 days postinoculation (dpi), and swabs and sections from sinuses, tracheas, and lungs were collected at necropsy. Viral titers in sinuses, tracheas, and lungs were determined by $TCID_{50}$, and viral RNA burden was quantified by real-time RT-PCR (Table 1).

(i) Clinical signs. At dpi 3, all turkey poults inoculated with raMPV-CO exhibited typical clinical signs of aMPV infection, including cough, turbid nasal exudates, frothy eyes, and/or swollen infraorbital sinuses. The clinical signs persisted until 10 dpi. In contrast, turkey poults inoculated with raMPV-G1696A, -G1700A, -N1701A, and -D1755A did not have significant clinical signs during the course of the experimental period. Turkeys in the uninfected control group had no clinical signs. Therefore, all raMPV mutants are avirulent to turkey poults.

(ii) Virus titer. At dpi 3, all 3 turkeys infected with raMPV-CO had a high titer of infectious virus. Virus titers in sinus and trachea swabs were 4.75 and 5.25 $\log_{10}$ $TCID_{50}$/ml, respectively. Although all turkeys inoculated with raMPV-G1696A and -G1700A were aMPV positive, the virus titer was significantly less than that in the raMPV group. For raMPV-G1696A, 3.50 and 3.25 $\log_{10}$ $TCID_{50}$/ml virus were detected in sinus and trachea, respectively. For raMPV-G1700A, 4.00 and 4.25 $\log_{10}$ $TCID_{50}$/ml virus were found in sinus and trachea, respectively. Two out of three turkeys in raMPV-N1701A- and -D1755A-infected groups had infectious viruses. Viral titers in sinus and trachea were 2.0 to 2.5 and 3 to 3.25 $\log_{10}$ $TCID_{50}$/ml less than those in the raMPV group, respectively. Under our experimental conditions, no infectious virus was detected in lungs from any virus-infected group. At dpi 5, two out of three turkeys had infectious virus in sinus, with an average titer of 2.5 $\log_{10}$ $TCID_{50}$/ml, and one out of three turkeys had infectious virus in the trachea, with a titer of 2.75 $\log_{10}$ $TCID_{50}$/ml. In contrast, turkeys in all raMPV mutant-infected groups had no detectable virus. At dpi 7 and dpi 10, all virus-infected groups were virus negative. Overall, raMPV-G1696A and -G1700A were moderately (1.2-log defects) attenuated in virus replication in turkeys,

TABLE 1 Replication of raMPV mutants in the upper and lower respiratory tracts of turkeys

Date postinoculation and inoculum[a]	Clinical signs ($n = 3$)[c]	Virus replication in:[b]								
		Sinus (n = 3)			Trachea ($n = 3$)			Lung ($n = 3$)		
		No. of infected animals[d]	Viral titer (log_{10} $TCID_{50}$/ml)	Viral RNA (log_{10} GRC/ml)[e]	No. of infected animals	Viral titer (log_{10} $TCID_{50}$/ml)	Viral RNA (log_{10} GRC/ml)	No. of infected animals	Viral titer (log_{10} $TCID_{50}$/g)	Viral RNA (log_{10} GRC/g)
Day 3										
raMPV-CO	3	3	4.75 ± 0.25 A	6.78 ± 0.01 A	3	5.25 ± 0.38 A	7.11 ± 0.03 A	0	ND	7.36 ± 0.28 A
G1696A	0	3	3.50 ± 0.20 B	6.00 ± 0.37 B	3	3.25 ± 0.46 C	6.19 ± 0.01 B	0	ND	6.18 ± 0.05 B
G1700A	0	3	4.00 ± 0.19 B	6.22 ± 0.01 B	3	4.25 ± 0.13 B	6.25 ± 0.14 B	0	ND	6.16 ± 0.04 B
N1701A	0	2	2.75 ± 0.10 C	6.17 ± 0.04 B	2	2.25 ± 0.38 C	6.16 ± 0.05 B	0	ND	6.05 ± 0.03 B
D1755A	0	2	2.25 ± 0.26 C	6.20 ± 0.15 B	2	2.00 ± 0.39 C	6.21 ± 0.03 B	0	ND	6.12 ± 0.06 B
DMEM	0	0	ND	ND	0	ND	ND	0	ND	ND
Day 5										
raMPV-CO	3	2	2.50 ± 0.38	6.00 ± 0.18 A	1	2.75 ± 0.00	6.85 ± 0.25 A	0	ND	6.24 ± 0.13 A
G1696A	0	0	ND	4.68 ± 1.06 B	0	ND	4.48 ± 0.05 B	0	ND	4.99 ± 1.24 B
G1700A	0	0	ND	5.29 ± 0.18 B	0	ND	5.87 ± 2.09 B	0	ND	5.37 ± 1.72 B
N1701A	0	0	ND	4.14 ± 0.46 C	0	ND	3.84 ± 0.33 C	0	ND	4.78 ± 0.70 B
D1755A	0	0	ND	3.64 ± 2.24 C	0	ND	3.83 ± 0.11 C	0	ND	4.18 ± 2.04 C
DMEM	0	0	ND	ND	0	ND	ND	0	ND	ND
Day 7										
raMPV-CO	3	0	ND	4.12 ± 0.21 A	0	ND	3.99 ± 0.05 A	0	ND	4.15 ± 0.15 A
G1696A	0	0	ND	3.45 ± 0.03 B	0	ND	3.12 ± 0.15 B	0	ND	5.42 ± 0.04 A
G1700A	0	0	ND	4.02 ± 0.21 A	0	ND	3.78 ± 0.33 A	0	ND	3.55 ± 0.28 B
N1701A	0	0	ND	2.30 ± 0.15 C	0	ND	2.55 ± 0.31 C	0	ND	2.90 ± 0.38 C
D1755A	0	0	ND	2.00 ± 0.06 C	0	ND	2.12 ± 0.23 C	0	ND	2.43 ± 0.04 C
DMEM	0	0	ND	ND	0	ND	ND	0	ND	ND
Day 10										
raMPV-CO	0	0	ND	3.02 ± 0.11 A	0	ND	2.99 ± 0.23 A	0	ND	3.15 ± 0.44 A
G1696A	0	0	ND	ND	0	ND	ND	0	ND	ND
G1700A	0	0	ND	2.49 ± 1.14 B	0	ND	2.25 ± 0.33 B	0	ND	2.18 ± 0.13 B
N1701A	0	0	ND	ND	0	ND	ND	0	ND	ND
D1755A	0	0	ND	ND	0	ND	ND	0	ND	ND
DMEM	0	0	ND	ND	0	ND	ND	0	ND	ND

[a] Two-week-old SPF turkeys were inoculated intranasally with DMEM as a control or with 2×10^5 $TCID_{50}$ of raMPV-CO or a mutant virus. At days 3, 5, 7, and 10 postinoculation, three animals in each group were euthanized for viral isolation.

[b] Titers are the average values for virus-positive animals. Values within a column for the same day followed by different letters (A, B, and C) are significantly different ($P < 0.05$). *n*, number of animals per group; ND, not detectable.

[c] The number of turkeys with clinical signs of aMPV infection.

[d] Turkeys that had infectious virus particles were reported as infected animals.

[e] GRC, indicates genomic RNA copies.

TABLE 2 Histologic changes caused by MTase-defective raMPVs

Inoculum[a]	Histological findings in:			
	Trachea		Lung	
	No. of turkeys with lesion ($n = 3$)[b]	Avg score[c]	No. turkeys with lesion ($n = 3$)	Avg score
DMEM	0	0	0	0
raMPV-CO	3	2.5 A	3	2.5 A
G1696A	3	1.0 B	2	1.0 B
G1700A	2	0.67 B	2	0.67 B
N1701A	2	0.67 B	1	0.33 B
D1755A	2	0.67 B	1	0.33 B

[a] raMPV-CO virus or the indicated mutant. DMEM was used as a control.
[b] *n*, number of animals per group.
[c] The severity of histologic change was scored for each trachea and lung tissue sample. Average score for each group is indicated as follows: 0, no change; 1, mild change; 2, moderate change; 3, severe change. Values within a column followed by the different letters (A and B) are significantly different ($P < 0.05$).

whereas raMPV-N1701A and -D1755A were highly (more than 3-log defects) attenuated in virus replication.

(iii) Viral RNA. Viral genomic RNA burden was quantitated by real-time RT-PCR. At dpi 3, all samples from sinus, trachea, and lung were RNA positive. raMPV mutant groups had 0.5 to 0.8 log, 0.8 to 1.0 log, and 1.2 to 1.4 logs fewer genomic RNA copies in sinus, trachea, and lung, respectively, than raMPV. At dpi 5, raMPV mutant groups had 0.7 to 2.4 logs, 1.0 to 3.0 logs, and 1.3 to 2.0 logs fewer genomic RNA copies in sinus, trachea, and lung, respectively. At dpi 10, the raMPV-CO group had 2 to 3 logs RNA whereas raMPV-G1696A, -N1701A, and -D1755A groups were RNA negative. Consistent with virus replication data, raMPV-G1696A and -G1700A were moderately attenuated in genomic RNA replication in turkeys, whereas raMPV-N1701A and -D1755A were highly (more than 3-log defects) attenuated in RNA replication.

(iv) Genetic stability. The CR VI of the L gene from sinus, trachea, and lung samples of each turkey was amplified by RT-PCR, and sequence analysis confirmed the presence of the mutation in all raMPV mutants. In addition, viral genome from lung tissue was amplified by RT-PCR and sequenced. No additional mutations were found in the genome except for the desired mutation in the MTase region of the L gene. This indicates that MTase-defective raMPV mutants remained genetically stable in turkeys.

(v) Histologic findings. All trachea and lung tissues at dpi 3 were examined for histologic changes. As shown in Table 2 and Fig. 6, trachea tissues from the raMPV-CO-inoculated group had moderate to severe histological changes characterized by tracheal epithelial cell necrosis or loss, mucus secretion, and inflammation. In addition, lungs from the raMPV-CO-inoculated group had moderate to severe histological changes characterized by bronchial epithelial and alveolar cell necrosis or loss, mucus secretion, excess layered mucus, and inflammatory cell infiltrates. In contrast, tracheal and lung tissues from all raMPV mutant groups exhibited only mild histologic changes. No histologic change was found in the uninfected control group. These results further suggest that raMPV mutants were attenuated in turkeys.

Turkey poults vaccinated with raMPV mutants provided complete protection against challenge with a homologous aMPV-CO strain. Next, we determined whether turkeys vaccinated with raMPV mutants can induce protective immunity. Briefly, 1-week-old turkey poults were vaccinated with each raMPV mutant were challenged with a virulent raMPV-CO strain at week 3 postvaccination. At 3, 5, 7, and 10 days postchallenge (dpc), 5 turkeys from each group were euthanized; infectious virus and viral RNA in sinus, trachea, and lung were quantified by $TCID_{50}$ and real-time RT-PCR, respectively (Table 3).

(i) Virus-serum neutralizing antibody titer. At week 3 postvaccination, serum samples were collected from each turkey, and the virus-serum neutralizing antibody was determined. As shown

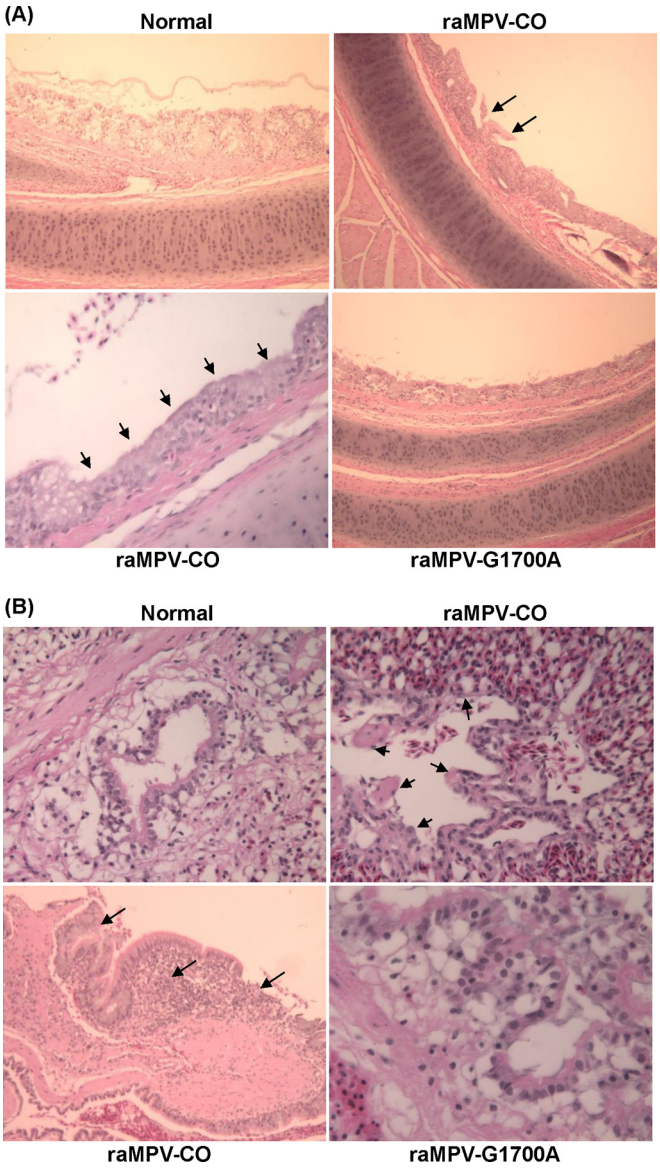

FIG 6 Trachea and lung histological changes in turkeys infected by MTase-defective raMPVs. Trachea and right lung from each turkey was preserved in 4% (vol/vol) phosphate-buffered paraformaldehyde. Fixed tissues were embedded in paraffin, sectioned at 5 μm, and stained with hematoxylin-eosin (H&E) for the examination of histological changes by light microscopy. Arrows indicates the histologic changes. (A) Histology of trachea tissue. Trachea tissues from raMPV-CO group had epithelial cell necrosis or loss, cilia loss, and inflammation. Magnification, ×100. (B) Histology of lung tissue. Lung tissues from raMPV-CO had bronchial epithelial and alveolar cell necrosis or loss, mucus secretion, and inflammatory cell infiltrates. Magnification, ×200.

TABLE 3 Protection efficacy of aMPV mutants against the challenge of raMPV-CO strain

Date postchallenge and inoculum[a]	Clinical signs ($n = 5$)[c]	Virus replication in:[b]								
		Sinus ($n = 5$)			Trachea ($n = 5$)			Lung ($n = 5$)		
		No. of infected animals[d]	Viral titer (log_{10} $TCID_{50}$/ml)	Viral RNA (log_{10} GRC/ml)[e]	No. of infected animals	Viral titer (log_{10} $TCID_{50}$/ml)	Viral RNA (log_{10} GRC/ml)	No. of infected animals	Viral titer (log_{10} $TCID_{50}$/g)	Viral RNA (log_{10} GRC/g)
Day 3										
DMEM	5	5	5.25 ± 0.23 A	6.17 ± 0.28 A	5	4.95 ± 0.13 A	6.67 ± 0.15 A	0	ND	7.54 ± 0.35 A
DMEMC	0	0	ND	ND	0	ND	ND	0	ND	ND
raMPV-CO	0	2	2.25 ± 0.16 B	4.92 ± 0.12 B	2	2.75 ± 0.00 B	4.12 ± 0.11 B	0	ND	4.36 ± 0.33 B
G1696A	0	0	ND	3.34 ± 0.08 C	0	ND	2.96 ± 0.10 C	0	ND	3.77 ± 0.10 B
G1700A	0	0	ND	3.84 ± 0.16 C	0	ND	3.61 ± 0.73 B	0	ND	3.96 ± 0.66 B
N1701A	0	0	ND	3.92 ± 0.19 C	0	ND	3.73 ± 0.46 B	0	ND	3.78 ± 0.49 B
D1755A	0	1	2.05 ± 0.00 B	3.94 ± 0.04 C	1	2.05 ± 0.00 B	3.43 ± 0.41 B	0	ND	3.65 ± 0.18 B
Day 5								0		
DMEM	5	2	2.75 ± 0.00	5.11 ± 0.03 A	2	2.25 ± 0.00	5.02 ± 0.10 A	0	ND	5.37 ± 0.14 A
DMEMC	0	0	ND	ND	0	ND	ND	0	ND	ND
raMPV-CO	0	0	ND	2.69 ± 0.23 B	0	ND	2.62 ± 1.32 B	0	ND	3.37 ± 0.48 B
G1696A	0	0	ND	2.20 ± 1.83 B	0	ND	2.29 ± 0.40 B	0	ND	2.51 ± 0.73 C
G1700A	0	0	ND	2.50 ± 0.74 B	0	ND	2.41 ± 0.43 B	0	ND	2.87 ± 0.10 C
N1701A	0	0	ND	2.12 ± 0.00 B	0	ND	2.03 ± 0.00 B	0	ND	2.21 ± 0.23 C
D1755A	0	0	ND	1.97 ± 0.33 B	0	ND	2.18 ± 0.71 B	0	ND	2.19 ± 0.41 C
Day 7		0			0					
DMEM	5	0	ND	4.07 ± 0.41	0	ND	4.18 ± 0.08	0	ND	4.87 ± 0.11 A
DMEMC	0	0	ND	ND	0	ND	ND	0	ND	ND
raMPV-CO	0	0	ND	ND	0	ND	ND	0	ND	ND
G1696A	0	0	ND	ND	0	ND	ND	0	ND	ND
G1700A	0	0	ND	ND	0	ND	ND	0	ND	ND
N1701A	0	0	ND	ND	0	ND	ND	0	ND	1.19 ± 0.00 B
D1755A	0	0	ND	ND	0	ND	ND	0	ND	1.01 ± 0.00 B

[a] Two-week-old SPF turkeys were immunized intranasally with DMEM or 2×10^5 $TCID_{50}$ of raMPV-CO or mutant virus. At week 4 postimmunization, each group was challenged with the raMPV-CO strain. At days 3, 5, and 7 postchallenge, 5 animals in each group were euthanized for viral isolation. DMEM, unvaccinated challenge control; DMEMC, unvaccinated unchallenged control.

[b] Titers are average values for virus-positive animals. Values within a column for the same day followed by different letters (A, B, and C) are significantly different ($P < 0.05$). ND, not detectable; *n*, number of animals per group.

[c] The number of turkeys with clinical signs of aMPV infection.

[d] Turkeys that had infectious virus particles were reported as infected animals.

[e] GRC, genomic RNA copies.

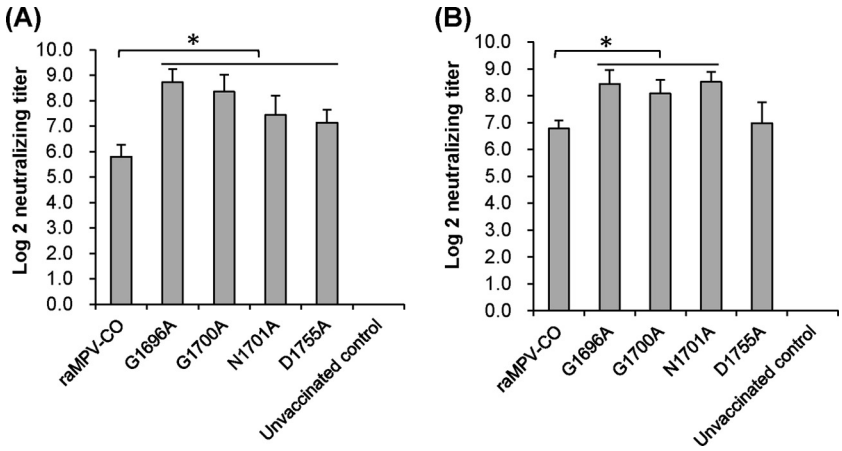

FIG 7 Recombinant aMPVs triggered a high level of neutralizing antibody titer in turkeys. Turkey poults were immunized with each recombinant aMPV intranasally at a dose of 2.0×10^5 PFU per turkey. Blood samples were collected at week 3 postvaccination. The aMPV neutralizing antibody was determined using a plaque reduction neutralization assay as described in Materials and Methods. Average titers for each group are shown. (A) Antibody responses in turkeys from animal experiment 2. (B) Antibody responses in turkeys from animal experiment 3.

in Fig. 7A, all aMPV mutants triggered high levels of antibody. Importantly, antibody titers in aMPV mutant groups were significantly higher than those infected by raMPV-CO. No antibody was detected in the unvaccinated controls. Thus, these data demonstrated that MTase-defective raMPVs were highly capable of eliciting antibody responses even though they were attenuated in turkeys.

(ii) Clinical signs. At dpc 3, all turkey poults in the unvaccinated challenged control group had typical clinical signs for aMPV infection, which persisted until dpc 7. In contrast, turkey poults vaccinated with raMPV-CO, raMPV-G1696A, -G1700A, -N1701A, and -D1755A did not have clinical signs during the course of the experimental period. In addition, turkeys in the unchallenged control group had no clinical signs. Therefore, turkeys vaccinated with the raMPV mutant were protected from clinical signs of aMPV infection.

(iii) Viral titer. At dpc 3, all turkeys in the unvaccinated challenged control group had infectious virus in sinus and trachea, with an average titer of 5.25 and 4.95 $\log_{10}$ $TCID_{50}$/ml, respectively. Two out of five turkeys vaccinated in the raMPV-CO group had 2.25 and 2.75 $\log_{10}$ $TCID_{50}$/ml of infectious virus in sinus and trachea, respectively. One out of five turkeys vaccinated with raMPV-D1755A had 2.05 $\log_{10}$ $TCID_{50}$/ml of infectious virus in both sinus and trachea. No infectious virus was detected in sinus and trachea in raMPV-G1696A-, -G1700A-, and -N1701A-vaccinated groups. No virus was detected in lungs of any group. At 5 dpc, all vaccinated groups were negative for infectious virus, whereas the unvaccinated challenged controls had 2.75 and 2.25 $\log_{10}$ $TCID_{50}$/ml infectious virus in sinus and trachea, respectively. At dpc 7, all groups were negative for aMPV. Therefore, vaccination of each raMPV mutant protected against viral replication in sinus and trachea in turkeys.

(iv) Viral RNA. At dpc 3, unvaccinated challenged control birds had 6.17 logs, 6.67 logs, and 7.54 logs of RNA copies in sinus, trachea, and lung, respectively. In contrast, all vaccinated groups had 3- to 4-log reductions in RNA copies in sinus, trachea, and lung. Similarly, at dpc 5, all vaccinated groups had 3-log defects in RNA copies compared to unvaccinated challenged controls. At dpc 7, unvaccinated challenged controls had 4 logs of RNA copies, whereas all vaccinated groups were RNA negative. No RNA was detected in the normal control group. Therefore, these results demonstrated that turkeys vaccinated with raMPV-CO mutants

TABLE 4 Summary of phenotype of MTase-defective raMPVs

Vaccine strain	Attenuation in cell culture[a]	Attenuation in turkeys[b]	Protection against aMPV-CO[c]				Protection against aMPV-MN			
			No. of protected animals ($n = 5$)[d]			Overall protection rate (%)[e]	No. of protected animals ($n = 5$)			Overall protection rate (%)
			Day 3	Day 5	Day 7		Day 3	Day 5	Day 7	
raMPV-CO	NA	Virulent	3	5	5	86.7	1	5	5	73.3
G1696A	Attenuated	Moderately attenuated	5	5	5	100	5	5	5	100
G1700A	Attenuated	Moderately attenuated	5	5	5	100	5	5	5	100
N1701A	Attenuated	Highlyattenuated	5	5	5	100	5	5	5	100
D1755A	Attenuated	Highlyattenuated	4	5	5	93.3	1	5	5	73.3

[a] Attenuation in cell culture was based on viral plaque morphology and cytopathic effect.
[b] Attenuation was based on virus replication, RNA replication, and lung and trachea histology.
[c] At week 3 postvaccination, turkeys were challenged with the aMPV-CO strain. At days 3, 5, and 7 postchallenge, five turkeys from each group were euthanized. Protection was based on the lack of clinical signs and on viral replication in sinus, trachea, and lungs.
[d] *n*, number of animals per group.
[e] The protection rate was calculated based on a total of 15 turkeys used for each vaccine group.

were completely protected against challenge with the homologous aMPV CO strain (Table 4).

Vaccination of turkey poults with raMPV mutants provided complete protection against challenge with a heterologous aMPV MN strain. We also determined whether turkeys vaccinated with raMPV mutants could be protected against challenge with a heterologous aMPV MN strain. As shown in Fig. 7B, virus-serum neutralizing antibody titers in raMPV-G1696A, -G1700A, and -N1701A groups were significantly higher than the titer in raMPV-CO group ($P < 0.05$). As shown in Table 5, the results were essentially similar to what was observed for a challenge experiment using the raMPV-CO strain. Unvaccinated turkeys challenged with the aMPV-MN strain exhibited clinical signs of aMPV infection, whereas all vaccinated groups lacked clinical signs. No infectious virus was detected in turkeys vaccinated with aMPV-G1696A, -G1700A, and -N1701A at dpc 3, 5, and 7. Four out of five turkeys in the raMPV-CO and raMPV-D1755A groups at dpc 3 were aMPV positive. However, significantly less virus (2 to 3 logs) was detected in sinus and trachea in turkeys vaccinated with raMPV-CO and raMPV-D1755A at dpc 3. In addition, turkeys vaccinated with raMPV mutants had 3 to 4 logs fewer RNA copies than the unvaccinated challenged controls at dpc 3 and dpc 5. No RNA was detectable in vaccinated groups at dpc 7, whereas approximately 4 log RNA copies remained in the unvaccinated controls. Collectively, these results demonstrated that turkeys vaccinated with raMPV-G1696A, -G1700A, and -N1701A were completely protected against challenge with the heterologous aMPV MN strain (Table 4).

DISCUSSION

In this study, we generated four recombinant viruses with amino acid substitutions in the predicted SAM binding site and examined the effects of these mutations on viral mRNA cap methylation, pathogenesis, and immunogenicity. We found that amino acid residues in G1696, G1700, N1701, and D1755 within the SAM binding site were essential for 2′-O methylation and that recombinant aMPVs carrying these mutations were highly attenuated in cell culture as well as in turkeys. Importantly, a single-dose vaccination of turkeys with these attenuated raMPV mutants provided complete protection against the challenge with homologous and heterologous aMPV strains. To our knowledge, this is first demonstration of the safety and efficacy of 2′-*O* MTase-defective recombinant viruses in the natural hosts.

2′-*O* MTase is a novel target for attenuation of aMPV and other RNA viruses. Avian paramyxoviruses include many economically important pathogens. Within the genus *Avulavirus* in the subfamily of *Paramyxovirinae*, at least 11 distinct serotypes of avian paramyxoviruses (named APMV 1 to 11) have been identified (38). APMV-1, also known as Newcastle disease virus (NDV), is responsible for one of the most disastrous diseases in birds and is considered a major economic threat to the poultry industry worldwide (39). Another important avian paramyxovirus is aMPV, which is in the genus *Metapneumovirus* in the subfamily *Pneumovirinae*. Since the discovery of aMPV in 1970, live attenuated vaccines have been developed for aMPV types A and B in Europe (21, 40). After the detection of an aMPV subtype C in the United States, a live attenuated vaccine has also been developed (41). These vaccine strains were generated by blind passage of the virulent strains in tissue culture. In some cases, serial passage of aMPV in cell culture led to truncation of viral G protein, raising the concern of genetic stability of the virus (40, 42–45). Virulence reversion is another major risk for using these attenuated vaccines. In fact, outbreaks of aMPV due to virulence reversion of live aMPV vaccines have been reported in Europe (22, 23). More recently, reverse-genetics systems for aMPV, whereby infectious virus is derived from cDNAs, has facilitated the development of new live attenuated aMPV vaccine candidates. Traditional attenuation strategies for paramyxoviruses have been focused on engineering mutations in two glycoproteins (F or HN/G proteins) (42). However, both F and HN/G proteins are viral immunogenic antigens that are responsible for protective immunity (46). As a consequence, mutations in glycoproteins will likely impair the immunogenicity of the attenuated live vaccine. In addition, a gene deletion mutant has been proposed to attenuate the aMPV. However, it was shown that deletion of individual nonessential genes (SH, G, and M2-2) in aMPV type A virus severely impaired antibody response, protection, and immunogenicity (42, 47, 48). Therefore, exploration of new attenuation targets to generate more stable and efficacious vaccines is urgently needed.

We hypothesize that the viral mRNA cap MTase is an excellent target to rationally attenuate aMPV for the development of live attenuated vaccines. We found that 2′-*O* MTase-defective raMPVs were attenuated in cell culture, as judged by diminished viral plaque size and delayed CPE (Table 4). *In vivo*, we found that 2′-*O* MTase-defective raMPVs were attenuated in viral replication in the upper and lower respiratory tract of turkeys (Table 4). Specifically, raMPV-D1755A and raMPV-N1701A were highly attenuated in virus replication *in vivo*. No infectious virus particles were found in the upper or lower respiratory tracts in turkeys inoculated with these two raMPV mutants. Recombinant raMPV-G1696A and raMPV-G1700A were moderately attenuated, based on the evidence that two out of three animals had low levels of virus replication in tracheal and sinus swabs. Under our experimental conditions, we were not able to detect any infectious aMPV from lungs despite the fact that moderate to severe lung histological lesions were found in turkeys infected by both wild-type aMPV-CO and -MN strains. Failure to detect infectious virus in lungs may be due to variations in environmental factors (such as humidity), tissue homogenization methods, inhibitors in lung tissues, or the sensitivity of the $TCID_{50}$ assay. In fact, attempts have been made to improve the aMPV challenge model by coinfection of bacterial pathogens (1, 41). Previously, it was shown that these experimental factors dramatically affected viral titers of hMPV, another member in the genus *Metapneumovirus*, in lungs of mice (reviewed in reference 49). However, we showed that the levels of viral genomic RNA in lungs from MTase-defective raMPV groups were significantly lower than those from the raMPV group, further supporting the idea that MTase-defective raMPVs were attenuated in replication in lungs. In this study, we chose aMPV-CO and -MN strains as challenge viruses since they are the most representative of strains that are prevalent in the United States and have been widely used as virulent strains to evaluate the efficacy of aMPV vaccines (1, 41, 46). In addition, these two strains have significant amino acid variability (76.1% homology) in the attachment glycoprotein (G) although they share relatively high identity (98.7%) in the fusion (F) glycoprotein. Importantly, turkeys vaccinated with raMPV mutants (derived from the aMPV-CO strain) triggered a higher level of neutralizing antibody and were completely protected against challenge with the homologous aMPV-CO strain and heterolo-

TABLE 5 Protection efficacy of aMPV mutants against the challenge of aMPV-MN strain

Date postchallenge and inoculum[a]	Clinical signs ($n = 5$)[c]	Virus replication in:[b]								
		Sinus			Trachea			Lung		
		No. of infected animals[d]	Viral titer (log_{10} $TCID_{50}$/ml)	Viral RNA (log_{10} GRC/ml)[e]	No. of infected animals[d]	Viral titer (log_{10} $TCID_{50}$/ml)	Viral RNA (log_{10} GRC/ml)[e]	No. of infected animals[d]	Viral titer (log_{10} $TCID_{50}$/g)	Viral RNA (log_{10} GRC/g)[e]
Day 3										
DMEM	5	5	4.50 ± 0.78 A	6.02 ± 0.14 A	5	3.75 ± 0.17 A	6.98 ± 0.55 A	0	ND	7.14 ± 0.46 A
DMEMC	0	0	ND	ND	0	ND	ND	0	ND	ND
raMPV-CO	0	4	2.75 ± 0.22 B	3.78 ± 0.33 B	4	2.56 ± 0.93 B	3.02 ± 0.18 B	0	ND	3.96 ± 0.11 B
G1696A	0	0	ND	2.87 ± 0.83 C	0	ND	3.64 ± 0.11 B	0	ND	3.68 ± 0.77 B
G1700A	0	0	ND	3.81 ± 0.12 B	0	ND	3.74 ± 0.51 B	0	ND	3.86 ± 0.89 B
N1701A	0	0	ND	3.45 ± 1.47 B	0	ND	3.53 ± 0.26 B	0	ND	3.52 ± 0.16 B
D1755A	0	4	2.48 ± 1.32 B	3.58 ± 0.98 B	4	2.24 ± 0.28 B	3.43 ± 0.41 B	0	ND	3.48 ± 1.23 B
Day 5										
DMEM	5	2	2.50 ± 0.00	5.27 ± 1.13 A	2	2.00 ± 0.00	5.88 ± 0.34 A	0	ND	5.00 ± 0.53 A
DMEMC	0	0	ND	ND	0	ND	ND	0	ND	ND
raMPV-CO	0	0	ND	2.52 ± 1.34 B	0	ND	2.58 ± 0.01 B	0	ND	2.19 ± 0.21 B
G1696A	0	0	ND	2.15 ± 0.35 B	0	ND	2.13 ± 0.03 B	0	ND	2.20 ± 0.97 B
G1700A	0	0	ND	2.50 ± 0.45 B	0	ND	2.42 ± 0.75 B	0	ND	2.87 ± 0.71 B
N1701A	0	0	ND	2.08 ± 0.00 B	0	ND	2.13 ± 1.83 B	0	ND	2.17 ± 0.19 B
D1755A	0	0	ND	2.14 ± 0.00 B	0	ND	2.15 ± 0.00 B	0	ND	2.03 ± 0.40 B
Day 7										
DMEM	5	0	ND	4.18.±0.27	0	ND	4.01 ± 0.76	0	ND	3.92 ± 0.67 A
DMEMC	0	0	ND	ND	0	ND	ND	0	ND	ND
raMPV-CO	0	0	ND	ND	0	ND	ND	0	ND	ND
G1696A	0	0	ND	ND	0	ND	ND	0	ND	ND
G1700A	0	0	ND	ND	0	ND	ND	0	ND	ND
N1701A	0	0	ND	ND	0	ND	ND	0	ND	1.23 ± 0.07 B
D1755A	0	0	ND	ND	0	ND	ND	0	ND	1.04 ± 0.00 B

[a] Two-week-old SPF turkeys were immunized intranasally with DMEM or 2×10^5 $TCID_{50}$s of raMPV-CO or the indicated mutant. At week 4 postimmunization, each group was challenged with the aMPV-MN strain. At days 3, 5, and 7, postchallenge (dpc), five animals in each group were euthanized for viral isolation. DMEM, unvaccinated challenge control; DMEMC, unvaccinated unchallenged control.

[b] Titers are the average values from virus-positive animals. Values within a column for the same day followed by different letters (A, B, and C) are significantly different ($P < 0.05$). ND, not detectable; *n*, number of animals per group.

[c] The number of turkeys with clinical signs of aMPV infection.

[d] Turkeys that had infectious virus particles were reported as infected animals.

[e] GRC, genomic RNA copies.

gous aMPV-MN strain (Table 4). Importantly, all raMPV mutants were genetically stable when passaged 12 times in cell culture. The viral genome RNA was also isolated from lung tissue and sequenced. No additional mutations were found in the genome except for the desired mutation in the CR VI of the L gene. In addition, some of the raMPV mutants (raMPV-G1700A, -N1701A, and -G1696A) grew to higher than or similar titers as the wild-type aMPV. Thus, it is economically feasible for manufacture. These results demonstrated that MTase-defective viruses are excellent vaccine candidates for aMPV.

The concept of using MTase as a target to generate live attenuated vaccine has been recently documented in several other RNA viruses. Previously, we showed that rVSV lacking both G-N-7 and 2′-O methylations were highly attenuated, whereas rVSV lacking only G-N-7 methylation had low virulence in mouse models (30). A 2′-*O* MTase-defective dengue virus vaccine candidate was highly attenuated and immunogenic in mouse and macaque models (50). In addition, a single vaccination of 2′-*O* MTase-defective Japanese encephalitis virus (JEV), another flavivirus, provided protection against lethal challenge with JEV strains in mice (51). Also, severe acute respiratory syndrome (SARS) coronavirus lacking 2′-O methylation was attenuated and provided protection against lethal challenge in mouse models (52). Therefore, targeting 2′-O methylation may provide a novel and global strategy for rationally designing live attenuated vaccine candidates for many RNA viruses whose genomic RNA or mRNA is 2′-O methylated. Although these vaccine candidates are promising in rodent or nonhuman primate models, their safety and efficacy profile in natural hosts are unknown. Particularly, many live vaccine candidates for paramyxoviruses (such as RSV) were initially shown to be safe and immunogenic in animal models but often lacked satisfactory safety and efficacy in human clinical trials (53, 54). In this study, we found that 2′-*O* MTase-defective aMPVs were not only highly attenuated and genetically stable but also highly immunogenic in turkey poults. This was the first demonstration that 2′-*O* MTase-defective viruses are safe and immunogenic in a natural host of a virus. This finding will facilitate the commercialization of MTase-defective live vaccine candidates in the future.

Mechanism of viral attenuation by inhibiting 2′-*O* MTase. Recently, many breakthroughs have been made in understanding the mechanism of virus attenuation by knocking out 2′-*O* MTase activity. It is known that G-N-7 methylation is essential for mRNA stability and efficient translation (reviewed in reference 55). Thus, abolishing G-N-7 methylation will inhibit the efficiency of viral protein translation, which in turn diminishes viral replication. This mechanism likely contributes to the attenuation of rVSV-G1670A and -G1672A which lacked G-N-7 but not 2′-O methylation. However, the biological function of 2′-O methylation remains elusive although it was discovered 4 decades ago. Recent studies in West Nile virus (WNV), mouse hepatitis virus (MHV), and vaccinia virus showed that 2′-O methylation is required to escape the interferon (IFN)-mediated innate immune response in host cells, and it functions as a molecular signature to discriminate self RNA from non-self RNA during viral infection (34, 56). At least two distinct antiviral mechanisms were affected by 2′-O-methylation. On one hand, human and mouse coronavirus mutants lacking 2′-*O* MTase activity induced higher expression of type I IFN and were highly sensitive to type I IFN. The induction of type I IFN by 2′-*O* MTase coronaviruses was dependent on the cytosolic innate immune receptor MDA5 (34). On the other hand, 2′-*O* MTase-defective WNV, MHV, and vaccinia virus were more sensitive to antiviral inhibition by IFN-inducible protein with tetratricopeptide repeats (IFITs), which are interferon-stimulated genes (ISGs) linked to translational regulation (56). It was also found that IFIT1 directly binds to the capped RNA and that this binding was dependent on the methylation state of the cap (57). Specifically, the binding of IFIT1 to 2′-O-unmethylated capped RNA impairs the recruitment of eukaryotic translation initiation factors to the 2′-O-unmethylated RNA template, thereby selectively inhibiting viral RNA translation. Collectively, the mechanism of attenuation of the 2′-*O* MTase viruses is attributable to the enhanced sensitivity to the antiviral action of IFN. Future experiments will aim to determine whether attenuation of 2′-*O* MTase-defective raMPVs is attributable to the IFN signaling pathways.

Mechanism of mRNA cap methylation in paramyxoviruses. The mechanism of paramyxovirus cap methylation is poorly understood, mostly due to lack of robust *in vitro* mRNA synthesis and the difficulty in purifying the L protein (24). Most of our knowledge on mRNA cap methylation comes from the studies of VSV, a rhabdovirus as prototype for NNS viruses. Previously, we showed that 2′-O methylation of VSV mRNA precedes and facilitates G-N-7 methylation, an order that is the reverse of all known mRNA cap methylations (29, 58). Mutations to the MTase catalytic site in the CR VI of L protein abolished both G-N-7 and 2′-O methylations, suggesting that G-N-7 and 2′-O methylation were carried out by a single CR VI (28). However, mutations in the SAM binding sites either diminished both G-N-7 and 2′-O methylation or specifically abolished G-N-7 methylation (29). Specifically, rVSV-G1670A and -G1672A were specifically defective in G-N-7, but not 2′-O, methylation. Recombinant rVSV-G1674A was not defective in either G-N-7 or 2′-O methylation but was sensitive to SAM concentration or *S*-adenosyl homocysteine (SAH) inhibition (29). Recombinant rVSV-D1735A was equally defective in both G-N-7 and 2′-O methylation (29). The fact that only one MTase catalytic site and one SAM binding site exist in the CR VI of the L protein of aMPV suggests that the general mechanism of mRNA cap methylation found in VSV may be conserved in aMPV. The equivalent amino acid residues G1670, G1674A, G1675A, and D1735A in VSV are G1696, G1700, N1701, and D1755 in hMPV, respectively (Fig. 1). In this study, we found that all raMPV mutants (G1696A, G1700A, N1701A, and D1755A) were defective in 2′-O, but not G-N-7, methylation, suggesting that G-N-7 methylation occurs prior to 2′-O methylation in aMPV. These results suggest that the order of mRNA cap methylation in paramyxoviruses may be different from that in VSV. This hypothesis was supported by a recent report showing that G-N-7 methylation of RSV occurs prior to 2′-O methylation (59). If a single SAM binding site is shared by both methylases, we expect that some mutations at this site would affect both G-N-7 and 2′-O, similar to what we observed in the VSV system. The question remains why G1696A, G1700A, N1701A, and D1755A affected only 2′-O and not G-N-7 methylation. Perhaps other amino acid residues with the G-rich motif may be required for G-N-7 methylation. For example, the role of amino acid residue G1698 and of amino acid residues (E1697 and A1699) flanking the G-rich motif in mRNA cap methylation is not known. In fact, our efforts to recover recombinant aMPVs carrying these amino acid changes were not successful. It is worth emphasizing that mutations to amino acid residues (D1671 and S1673) flanking the G-

rich motif in VSV L protein abolished both G-N-7 and 2′-O methylation (29, 60).

In summary, we showed that raMPVs defective in 2′-O methylation were sufficiently attenuated while retaining high immunogenicity in turkeys, the natural hosts of aMPV. Thus, 2′-*O* MTase-defective viruses are promising vaccine candidates for aMPV. This novel attenuation approach can potentially be used for other avian and human paramyxoviruses for vaccine purposes.

ACKNOWLEDGMENTS

This study was supported by grants from the USDA NIFA Animal Health Program (2010-65119-20602) and the NIH (R01AI090060) to J.L.

We thank Sean Whelan for MTase-defective VSVs. We thank Apath, LLC, for providing BHK-SR19-T7 cells. We thank Steven Krakowka for histology. We are grateful to members of the Li laboratory for critical readings of the manuscript.

REFERENCES

1. **Alkhalaf AN, Ward LA, Dearth RN, Saif YM.** 2002. Pathogenicity, transmissibility, and tissue distribution of avian pneumovirus in turkey poults. Avian Dis. **46:**650–659. http://dx.doi.org/10.1637/0005-2086(2002)046[0650:PTATDO]2.0.CO;2.
2. **Aung YH, Liman M, Neumann U, Rautenschlein S.** 2008. Reproducibility of swollen sinuses in broilers by experimental infection with avian metapneumovirus subtypes A and B of turkey origin and their comparative pathogenesis. Avian Pathol. **37:**65–74. http://dx.doi.org/10.1080/03079450701802222.
3. **Broor S, Bharaj P.** 2007. Avian and human metapneumovirus. Ann. N. Y. Acad. Sci. **1102:**66–85. http://dx.doi.org/10.1196/annals.1408.005.
4. **Padhi A, Poss M.** 2009. Population dynamics and rates of molecular evolution of a recently emerged paramyxovirus, avian metapneumovirus subtype C. J. Virol. **83:**2015–2019. http://dx.doi.org/10.1128/JVI.02047-08.
5. **Hafez HM, Hess M, Prusas C, Naylor CJ, Cavanagh D.** 2000. Presence of avian pneumovirus type A in continental Europe during the 1980s. J. Vet. Med. B Infect. Dis. Vet. Public Health **47:**629–633. http://dx.doi.org/10.1046/j.1439-0450.2000.00398.x.
6. **Toquin D, Guionie O, Jestin V, Zwingelstein F, Allee C, Eterradossi N.** 2006. European and American subgroup C isolates of avian metapneumovirus belong to different genetic lineages. Virus Genes **32:**97–103. http://dx.doi.org/10.1007/s11262-005-5850-3.
7. **Owoade AA, Ducatez MF, Hubschen JM, Sausy A, Chen H, Guan Y, Muller CP.** 2008. Avian metapneumovirus subtype A in China and subtypes A and B in Nigeria. Avian Dis. **52:**502–506. http://dx.doi.org/10.1637/8266-021208-Reg.1.
8. **Wei L, Zhu S, Yan X, Wang J, Zhang C, Liu S, She R, Hu F, Quan R, Liu J.** 2013. Avian metapneumovirus subgroup C infection in chickens, China. Emerg. Infect. Dis. **19:**1092–1094. http://dx.doi.org/10.3201/eid1907.121126.
9. **Seal BS.** 1998. Matrix protein gene nucleotide and predicted amino acid sequence demonstrate that the first US avian pneumovirus isolate is distinct from European strains. Virus Res. **58:**45–52. http://dx.doi.org/10.1016/S0168-1702(98)00098-7.
10. **Goyal SM, Chiang SJ, Dar AM, Nagaraja KV, Shaw DP, Halvorson DA, Kapur V.** 2000. Isolation of avian pneumovirus from an outbreak of respiratory illness in Minnesota turkeys. J. Vet. Diagn. Invest. **12:**166–168. http://dx.doi.org/10.1177/104063870001200214.
11. **Govindarajan D, Buchholz UJ, Samal SK.** 2006. Recovery of avian metapneumovirus subgroup C from cDNA: cross-recognition of avian and human metapneumovirus support proteins. J. Virol. **80:**5790–5797. http://dx.doi.org/10.1128/JVI.00138-06.
12. **Cha RM, Yu Q, Zsak L.** 2013. The pathogenicity of avian metapneumovirus subtype C wild bird isolates in domestic turkeys. Virol. J. **10:**38. http://dx.doi.org/10.1186/1743-422X-10-38.
13. **Turpin EA, Stallknecht DE, Slemons RD, Zsak L, Swayne DE.** 2008. Evidence of avian metapneumovirus subtype C infection of wild birds in Georgia, South Carolina, Arkansas and Ohio, U. S. A. Avian Pathol. **37:**343–351. http://dx.doi.org/10.1080/03079450802068566.
14. **van den Hoogen BG, de Jong JC, Groen J, Kuiken T, de Groot R, Fouchier RA, Osterhaus AD.** 2001. A newly discovered human pneumovirus isolated from young children with respiratory tract disease. Nat. Med. **7:**719–724. http://dx.doi.org/10.1038/89098.
15. **van den Hoogen BG, Herfst S, Sprong L, Cane PA, Forleo-Neto E, de Swart RL, Osterhaus AD, Fouchier RA.** 2004. Antigenic and genetic variability of human metapneumoviruses. Emerg. Infect. Dis. **10:**658–666. http://dx.doi.org/10.3201/eid1004.030393.
16. **Wei Y, Feng K, Yao X, Cai H, Li J, Mirza AM, Iorio RM, Li J.** 2012. Localization of a region in the fusion protein of avian metapneumovirus that modulates cell-cell fusion. J. Virol. **86:**11800–11814. http://dx.doi.org/10.1128/JVI.00232-12.
17. **Velayudhan BT, Nagaraja KV, Thachil AJ, Shaw DP, Gray GC, Halvorson DA.** 2006. Human metapneumovirus in turkey poults. Emerg. Infect. Dis. **12:**1853–1859. http://dx.doi.org/10.3201/eid1212.060450.
18. **Easton AJ, Domachowske JB, Rosenberg HF.** 2004. Animal pneumoviruses: molecular genetics and pathogenesis. Clin. Microbiol. Rev. **17:**390–412. http://dx.doi.org/10.1128/CMR.17.2.390-412.2004.
19. **Patnayak DP, Sheikh AM, Gulati BR, Goyal SM.** 2002. Experimental and field evaluation of a live vaccine against avian pneumovirus. Avian Pathol. **31:**377–382. http://dx.doi.org/10.1080/0307945022041651.
20. **Patnayak DP, Gulati BR, Sheikh AM, Goyal SM.** 2003. Cold adapted avian pneumovirus for use as live, attenuated vaccine in turkeys. Vaccine **21:**1371–1374. http://dx.doi.org/10.1016/S0264-410X(02)00722-3.
21. **Ganapathy K, Jones RC.** 2007. Vaccination of chicks with live attenuated subtype B avian metapneumovirus vaccines: protection against challenge and immune responses can be unrelated to vaccine dose. Avian Dis. **51:**733–737. http://dx.doi.org/10.1637/0005-2086(2007)51[733:VOCWLA]2.0.CO;2.
22. **Lupini C, Cecchinato M, Ricchizzi E, Naylor CJ, Catelli E.** 2011. A turkey rhinotracheitis outbreak caused by the environmental spread of a vaccine-derived avian metapneumovirus. Avian Pathol. **40:**525–530. http://dx.doi.org/10.1080/03079457.2011.607428.
23. **Catelli E, Cecchinato M, Savage CE, Jones RC, Naylor CJ.** 2006. Demonstration of loss of attenuation and extended field persistence of a live avian metapneumovirus vaccine. Vaccine **24:**6476–6482. http://dx.doi.org/10.1016/j.vaccine.2006.06.076.
24. **Whelan SP, Barr JN, Wertz GW.** 2004. Transcription and replication of nonsegmented negative-strand RNA viruses. Curr. Top. Microbiol. Immunol. **283:**61–119. http://dx.doi.org/10.1007/978-3-662-06099-5_3.
25. **Sleat DE, Banerjee AK.** 1993. Transcriptional activity and mutational analysis of recombinant vesicular stomatitis virus RNA polymerase. J. Virol. **67:**1334–1339.
26. **Li J, Rahmeh A, Morelli M, Whelan SP.** 2008. A conserved motif in region v of the large polymerase proteins of nonsegmented negative-sense RNA viruses that is essential for mRNA capping. J. Virol. **82:**775–784. http://dx.doi.org/10.1128/JVI.02107-07.
27. **Ogino T, Yadav SP, Banerjee AK.** 2010. Histidine-mediated RNA transfer to GDP for unique mRNA capping by vesicular stomatitis virus RNA polymerase. Proc. Natl. Acad. Sci. U. S. A. **107:**3463–3468. http://dx.doi.org/10.1073/pnas.0913083107.
28. **Li J, Fontaine-Rodriguez EC, Whelan SP.** 2005. Amino acid residues within conserved domain VI of the vesicular stomatitis virus large polymerase protein essential for mRNA cap methyltransferase activity. J. Virol. **79:**13373–13384. http://dx.doi.org/10.1128/JVI.79.21.13373-13384.2005.
29. **Li J, Wang JT, Whelan SP.** 2006. A unique strategy for mRNA cap methylation used by vesicular stomatitis virus. Proc. Natl. Acad. Sci. U. S. A. **103:**8493–8498. http://dx.doi.org/10.1073/pnas.0509821103.
30. **Ma Y, Wei Y, Zhang X, Zhang Y, Cai H, Zhu Y, Shilo K, Oglesbee M, Krakowka S, Whelan SP, Li J.** 2014. mRNA cap methylation influences pathogenesis of vesicular stomatitis virus in vivo. J. Virol. **88:**2913–2926. http://dx.doi.org/10.1128/JVI.03420-13.
31. **Yu Q, Estevez C, Song M, Kapczynski D, Zsak L.** 2010. Generation and biological assessment of recombinant avian metapneumovirus subgroup C (aMPV-C) viruses containing different length of the G gene. Virus Res. **147:**182–188. http://dx.doi.org/10.1016/j.virusres.2009.10.021.
32. **Reed LJ, Muench H.** 1938. A simple method of estimating fifty per cent endpoints. Am. J. Epidemiol. **27:**493–497.
33. **Zhang Y, Wei Y, Li J, Li J.** 2012. Development and optimization of a direct plaque assay for human and avian metapneumoviruses. J. Virol. Methods **185:**61–68. http://dx.doi.org/10.1016/j.jviromet.2012.05.030.
34. **Zust R, Cervantes-Barragan L, Habjan M, Maier R, Neuman BW, Ziebuhr J, Szretter KJ, Baker SC, Barchet W, Diamond MS, Siddell SG, Ludewig B, Thiel V.** 2011. Ribose 2′-O-methylation provides a molecular signature for the distinction of self and non-self mRNA dependent on the

RNA sensor Mda5. Nat. Immunol. **12:**137–143. http://dx.doi.org/10.1038/ni.1979.
35. **Wei Y, Zhang Y, Cai H, Mirza AM, Iorio RM, Peeples ME, Niewiesk S, Li J.** 2014. Roles of the putative integrin-binding motif of the human metapneumovirus fusion (F) protein in cell-cell fusion, viral infectivity, and pathogenesis. J. Virol. **88:**4338–4352. http://dx.doi.org/10.1128/JVI.03491-13.
36. **Bujnicki JM, Rychlewski L.** 2002. In silico identification, structure prediction and phylogenetic analysis of the 2′-*O*-ribose (cap 1) methyltransferase domain in the large structural protein of ssRNA negative-strand viruses. Protein Eng. **15:**101–108. http://dx.doi.org/10.1093/protein/15.2.101.
37. **Hager J, Staker BL, Bugl H, Jakob U.** 2002. Active site in RrmJ, a heat shock-induced methyltransferase. J. Biol. Chem. **277:**41978–41986. http://dx.doi.org/10.1074/jbc.M205423200.
38. **Nayak B, Dias FM, Kumar S, Paldurai A, Collins PL, Samal SK.** 2012. Avian paramyxovirus serotypes 2-9 (APMV-2-9) vary in the ability to induce protective immunity in chickens against challenge with virulent Newcastle disease virus (APMV-1). Vaccine **30:**2220–2227. http://dx.doi.org/10.1016/j.vaccine.2011.12.090.
39. **Kim SH, Wanasen N, Paldurai A, Xiao S, Collins PL, Samal SK.** 2013. Newcastle disease virus fusion protein is the major contributor to protective immunity of genotype-matched vaccine. PLoS One **8:**e74022. http://dx.doi.org/10.1371/journal.pone.0074022.
40. **Cecchinato M, Catelli E, Lupini C, Ricchizzi E, Clubbe J, Battilani M, Naylor CJ.** 2010. Avian metapneumovirus (AMPV) attachment protein involvement in probable virus evolution concurrent with mass live vaccine introduction. Vet. Microbiol. **146:**24–34. http://dx.doi.org/10.1016/j.vetmic.2010.04.014.
41. **Velayudhan BT, Noll SL, Thachil AJ, Shaw DP, Goyal SM, Halvorson DA, Nagaraja KV.** 2007. Development of a vaccine-challenge model for avian metapneumovirus subtype C in turkeys. Vaccine **25:**1841–1847. http://dx.doi.org/10.1016/j.vaccine.2006.10.037.
42. **Naylor CJ, Ling R, Edworthy N, Savage CE, Easton AJ.** 2007. Avian metapneumovirus SH gene end and G protein mutations influence the level of protection of live-vaccine candidates. J. Gen. Virol. **88:**1767–1775. http://dx.doi.org/10.1099/vir.0.82755-0.
43. **Chockalingam AK, Chander Y, Halvorson DA, Goyal SM.** 2010. Stability of the glycoprotein gene of avian metapneumovirus (Canada goose isolate 15a/01) after serial passages in cell cultures. Avian Dis. **54:**915–918. http://dx.doi.org/10.1637/9016-081909-RESNOTE.1.
44. **Kong BW, Foster LK, Foster DN.** 2008. Species-specific deletion of the viral attachment glycoprotein of avian metapneumovirus. Virus Res. **132:**114–121. http://dx.doi.org/10.1016/j.virusres.2007.11.006.
45. **Velayudhan BT, Yu Q, Estevez CN, Nagaraja KV, Halvorson DA.** 2008. Glycoprotein gene truncation in avian metapneumovirus subtype C isolates from the United States. Virus Genes **37:**266–272. http://dx.doi.org/10.1007/s11262-008-0220-6.
46. **Govindarajan D, Kim SH, Samal SK.** 2010. Contribution of the attachment G glycoprotein to pathogenicity and immunogenicity of avian metapneumovirus subgroup C. Avian Dis. **54:**59–66. http://dx.doi.org/10.1637/8991-071409-Reg.1.
47. **Ling R, Sinkovic S, Toquin D, Guionie O, Eterradossi N, Easton AJ.** 2008. Deletion of the SH gene from avian metapneumovirus has a greater impact on virus production and immunogenicity in turkeys than deletion of the G gene or M2-2 open reading frame. J. Gen. Virol. **89:**525–533. http://dx.doi.org/10.1099/vir.0.83309-0.
48. **Yu Q, Estevez CN, Roth JP, Hu H, Zsak L.** 2011. Deletion of the M2-2 gene from avian metapneumovirus subgroup C impairs virus replication and immunogenicity in Turkeys. Virus Genes **42:**339–346. http://dx.doi.org/10.1007/s11262-011-0577-9.
49. **Schildgen O, Simon A, Williams J.** 2007. Animal models for human metapneumovirus (HMPV) infections. Vet. Res. **38:**117–126. http://dx.doi.org/10.1051/vetres:2006051.
50. **Zust R, Dong H, Li XF, Chang DC, Zhang B, Balakrishnan T, Toh YX, Jiang T, Li SH, Deng YQ, Ellis BR, Ellis EM, Poidinger M, Zolezzi F, Qin CF, Shi PY, Fink K.** 2013. Rational design of a live attenuated dengue vaccine: 2′-o-methyltransferase mutants are highly attenuated and immunogenic in mice and macaques. PLoS Pathog. **9:**e1003521. http://dx.doi.org/10.1371/journal.ppat.1003521.
51. **Li SH, Dong H, Li XF, Xie X, Zhao H, Deng YQ, Wang XY, Ye Q, Zhu SY, Wang HJ, Zhang B, Leng QB, Zuest R, Qin ED, Qin CF, Shi PY.** 2013. Rational design of a flavivirus vaccine by abolishing viral RNA 2′-*O* methylation. J. Virol. **87:**5812–5819. http://dx.doi.org/10.1128/JVI.02806-12.
52. **Menachery VD, Yount BL, Jr, Josset L, Gralinski LE, Scobey T, Agnihothram S, Katze MG, Baric RS.** 2014. Attenuation and restoration of severe acute respiratory syndrome coronavirus mutant lacking 2′-*O*-methyltransferase activity. J. Virol. **88:**4251–4264. http://dx.doi.org/10.1128/JVI.03571-13.
53. **Karron RA, Wright PF, Belshe RB, Thumar B, Casey R, Newman F, Polack FP, Randolph VB, Deatly A, Hackell J, Gruber W, Murphy BR, Collins PL.** 2005. Identification of a recombinant live attenuated respiratory syncytial virus vaccine candidate that is highly attenuated in infants. J. Infect. Dis. **191:**1093–1104. http://dx.doi.org/10.1086/427813.
54. **Schickli JH, Dubovsky F, Tang RS.** 2009. Challenges in developing a pediatric RSV vaccine. Hum. Vaccin. **5:**582–591. http://dx.doi.org/10.4161/hv.9131.
55. **Shuman S, Schwer B.** 1995. RNA capping enzyme and DNA ligase: a superfamily of covalent nucleotidyl transferases. Mol. Microbiol. **17:**405–410. http://dx.doi.org/10.1111/j.1365-2958.1995.mmi_17030405.x.
56. **Daffis S, Szretter KJ, Schriewer J, Li J, Youn S, Errett J, Lin TY, Schneller S, Zust R, Dong H, Thiel V, Sen GC, Fensterl V, Klimstra WB, Pierson TC, Buller RM, Gale M, Jr, Shi PY, Diamond MS.** 2010. 2′-O methylation of the viral mRNA cap evades host restriction by IFIT family members. Nature **468:**452–456. http://dx.doi.org/10.1038/nature09489.
57. **Kimura T, Katoh H, Kayama H, Saiga H, Okuyama M, Okamoto T, Umemoto E, Matsuura Y, Yamamoto M, Takeda K.** 2013. Ifit1 inhibits Japanese encephalitis virus replication through binding to 5′ capped 2′-*O* unmethylated RNA. J. Virol. **87:**9997–10003. http://dx.doi.org/10.1128/JVI.00883-13.
58. **Rahmeh AA, Li J, Kranzusch PJ, Whelan SP.** 2009. Ribose 2′-*O* methylation of the vesicular stomatitis virus mRNA cap precedes and facilitates subsequent guanine-N-7 methylation by the large polymerase protein. J. Virol. **83:**11043–11050. http://dx.doi.org/10.1128/JVI.01426-09.
59. **Liuzzi M, Mason SW, Cartier M, Lawetz C, McCollum RS, Dansereau N, Bolger G, Lapeyre N, Gaudette Y, Lagace L, Massariol MJ, Do F, Whitehead P, Lamarre L, Scouten E, Bordeleau J, Landry S, Rancourt J, Fazal G, Simoneau B.** 2005. Inhibitors of respiratory syncytial virus replication target cotranscriptional mRNA guanylylation by viral RNA-dependent RNA polymerase. J. Virol. **79:**13105–13115. http://dx.doi.org/10.1128/JVI.79.20.13105-13115.2005.
60. **Grdzelishvili VZ, Smallwood S, Tower D, Hall RL, Hunt DM, Moyer SA.** 2005. A single amino acid change in the L-polymerase protein of vesicular stomatitis virus completely abolishes viral mRNA cap methylation. J. Virol. **79:**7327–7337. http://dx.doi.org/10.1128/JVI.79.12.7327-7337.2005.